

Fairness Evaluation of Risk Estimation Models for Lung Cancer Screening

Shaurya **Gaur** ^{1,2}, Michel **Vitale** ^{1,3}, Alessa **Hering** ¹, Johan **Kwisthout** ², Colin **Jacobs** ¹, Lena **Philipp** ¹*,
Fennie **van der Graaf** ¹*,

1 Diagnostic Image Analysis Group, Department of Medical Imaging, Radboud University Medical Center, Nijmegen, the Netherlands

2 Department of Artificial Intelligence, Radboud University, Nijmegen, the Netherlands

3 Ethics of Healthcare Group, Department IQ Health, Radboud University Medical Center, Nijmegen, the Netherlands

arXiv:2512.22242 [cs.II] 23 Dec 2025

Abstract

Lung cancer is the leading cause of cancer-related mortality in adults worldwide. Screening high-risk individuals with annual low-dose CT (LDCT) can support earlier detection and reduce deaths, but widespread implementation may strain the already limited radiology workforce. Artificial intelligence (AI) models have shown potential in estimating lung cancer risk from LDCT scans. However, high-risk populations for lung cancer are diverse, and these models' performance across diverse demographic groups remains an open question. In this study, we drew on the considerations on confounding factors and ethically significant biases outlined in the JustEFAB framework to evaluate potential performance disparities and fairness in two deep learning risk estimation models for lung cancer screening: the Sybil lung cancer risk model and the Venkadesh21 nodule risk estimator. We also examined disparities in the PanCan2b logistic regression model recommended in the British Thoracic Society nodule management guideline. Both deep learning models were trained on data from the U.S.-based National Lung Screening Trial (NLST), and assessed on a held-out NLST validation set. We evaluated area under the ROC curve (AUROC), sensitivity, and specificity across demographic subgroups, and explored potential confounding from clinical risk factors. We observed a statistically significant AUROC difference in Sybil's performance between women (0.88, 95% CI: 0.86, 0.90) and men (0.81, 95% CI: 0.78, 0.84, $p < .001$). At 90% specificity, Venkadesh21 showed lower sensitivity for Black (0.39, 95% CI: 0.23, 0.59) than White participants (0.69, 95% CI: 0.65, 0.73). These differences were not explained by available clinical confounders and thus may be classified as unfair biases according to JustEFAB. Our findings highlight the importance of improving and monitoring model performance across underrepresented subgroups in lung cancer screening, as well as further research on algorithmic fairness in this field.

Keywords

Lung Cancer Screening, Pulmonary Nodule, Lung CT Scans, Deep Learning, Medical Imaging, Machine Learning, AI Bias, Subgroup Performance Analysis, Brock Model, Cancer Risk Estimation Models, Algorithmic Fairness, Ethically Significant Bias, AI for Screening, Confounder Assessment, JustEFAB, Fair ML, Responsible AI, Healthcare ML Algorithms, Clinical Decision Support Systems.

Article informations

<https://doi.org/10.59275/j.melba.2025-1e7f>

©2025 Gaur, Vitale, Hering, Kwisthout, Jacobs, Philipp, and van der Graaf. License: CC-BY 4.0

Volume 3, Received: 2025-04-18, Published 2025-11



Corresponding author: fennie.vandergraaf@radboudumc.nl

Special issue: Special issue on Fairness of AI in Medical Imaging (FAIMI)

Guest editors: Veronika Cheplygina, Aasa Feragen, Andrew King, Ben Glocker, Enzo Ferrante, Eike Petersen, Esther Puyol-Antón, Melanie Ganz-Benjaminsen

1. Introduction

Lung cancer is the leading cause of cancer-related death in adults worldwide. To treat lung cancer before it becomes

*. Contributed equally as last authors.

terminal (Newson, 2011), radiologists have explored the use of screenings on high-risk populations, collecting images of their lungs to assess cancer risk by detecting pulmonary nodules and assessing their risk of malignancy (Wille et al., 2016). Results from the U.S. National Lung Screening Trial (NLST) (National Lung Screening Trial Research Team et al., 2011) and the Dutch-Belgian NELSON trial (de Koning et al., 2020) found that lung cancer screening (LCS) with low-dose computed tomography (LDCT) scans can significantly reduce lung cancer mortality in a high-risk population. Findings like these have encouraged trials and adoptions of LCS programs around the world at both the regional and national level¹. However, considering a global shortage of radiologists (Konstantinidis, 2024), implementing LCS would exacerbate their already stressful workload (Bruls and Kwee, 2020), increasing the risk of burnout and potentially reducing accuracy (Harolds et al., 2016).

To reduce radiologist workloads, several artificial intelligence (AI) systems have been built to automatically detect (Hendrix et al., 2023), measure and classify nodules (Lancaster et al., 2025), and assess the risk of malignancy of nodules (Venkadesh et al., 2021) and of lung cancer in LDCT scans (Mikhael et al., 2023). These deep learning (DL) models are trained and evaluated on LDCT datasets from screening trials (National Lung Screening Trial Research Team et al., 2011; Wille et al., 2016) and have been shown to perform comparably to radiologists in nodule malignancy risk estimation (Venkadesh et al., 2021). Some models have even shown greater performance than the Brock model (Venkadesh et al., 2021), a nodule malignancy calculator based on various lung cancer risk factors which has been employed by radiologists in screening protocols (Lim et al., 2020; Baldwin, 2016).

However, AI systems have shown biases between demographic subgroups based on factors like race, sex, and socioeconomic status (Obermeyer et al., 2019; Seyyed-Kalantari et al., 2021), which could perpetuate historical inequalities in healthcare (Spencer et al., 2013). In particular, DL models have tended to show lower accuracy for groups with less representation in their development data, such as women and racial minority groups (Seyyed-Kalantari et al., 2021). These groups have also been underrepresented in LCS trials (National Lung Screening Trial Research Team et al., 2011; Wille et al., 2016) and sometimes even excluded from analysis (de Koning et al., 2020), often due to biased screening criteria. LCS protocols, like the 2013 US Preventative Services Task Force guidelines, chose who to screen based on risk factors like age (i.e. 55 – 80 years old) and smoking history (i.e. ≥ 30 pack-years of smoking) (Moyer, 2014). Studies have shown that these guidelines are biased against women and Black Americans, who are

less likely to clear the 30 pack-year threshold (Shum et al., 2024; Aredo et al., 2022). This is especially concerning since studies have observed rising lung cancer rates for women even with lower smoking rates (Siegfried, 2021) and a higher lung cancer risk for Black American men than men in other racial groups (de Groot et al., 2018).

Bias in model performance between groups can also result from decisions made during model development, such as the choice of input data, labels, network architecture, and the loss functions upon which to optimize a model (Ferrara, 2024; Narayanan, 2018). A model architecture may exhibit shortcut learning, or the ability to predict a demographic characteristic in a way that may lead to spurious correlations which could bias performance for certain subgroups (Brown et al., 2023). For example, Mikhael et al. (2023) demonstrated that the Sybil lung cancer risk estimation model was able to accurately classify a participant's sex, height, weight, and smoking status from an LDCT. Additionally, clinical decisions made based on model output, such as the threshold used to stratify risk scores as either benign or malignant, can lead to disparate impact between subgroups (Ferrara, 2024). In LCS, such biases could lead to the overestimation or underestimation of lung cancer risk. Overestimation can unnecessarily burden both participants and healthcare practitioners with further treatment, with the potential to result in overdiagnosis for a particular group. Conversely, underestimation can falsely flag people with lung cancer as low-risk, potentially barring them from life-saving treatment, increasing the risk of underdiagnosis for a community. These biases would not only materially harm the affected communities based on their demographics, but also reduce their trust in LCS (Newson, 2011).

Usually, these biases are considered to be *unfair* when they lead an AI model to systematic (and unwarranted) differences in behavior towards a specific demographic subgroup of participants. While bias can be observed statistically, algorithmic fairness depends on stakeholders' values and priorities (Narayanan, 2018). This has led to various fairness definitions and frameworks (Obermeyer et al., 2021; Mccradden et al., 2023), which prioritize equalizing different metrics between groups. For example, the Algorithmic Bias Playbook from Obermeyer et al. (2021) prioritizes examining the differences in probability calibration curves between subgroups and choosing fair labels for the prediction task. Alternatively, the JustEFAB framework from Mccradden et al. (2023) emphasizes defining biases based on metrics which would measure treatment outcomes. Instead of examining fairness between groups, some studies argue that fairness should be examined more on an individual level, and ensure similar cases are treated alike (Giovanola and Tiribelli, 2023). Multiple studies have demonstrated that metrics between different AI fairness frameworks can be conflicting, so a framework should be carefully chosen ac-

1. <https://www.lungcancerpolicynetwork.com/interactive-map-of-lung-cancer-screening/>

cording to its use case (Barocas et al., 2023; Chouldechova and Roth, 2020; Richardson and Gilbert, 2021).

Moreover, a fairness evaluation in healthcare must properly consider any links between demographic groups and clinical confounders. Jones et al. (2024) describes how medical imaging datasets often have demographic disparities in the prevalence of clinical risk factors, the presentation of medical images, and the annotation practices surrounding malignancy labels. These clinical disparities add a layer of dataset bias that may confound a performance disparity seen between subgroups (Bernhardt et al., 2022). To assess fairness based on these links, we must carefully examine their causality: if a demographic is clinically linked to a medical risk factor, it may be a fair bias, and this trait may be a useful predictor. This reflects how clinicians aim to use all of the information about a patient (including demographic traits) to gain valuable insights about their risk for disease (Giovanola and Tiribelli, 2023). Conversely, some prevalence links may be due to unfair selection biases, such as racial disparities in access to healthcare, which influence who in a particular group is more likely to have a medical image taken (Jones et al., 2024).

In this study, we were guided by the first part of the JustEFAB framework and its considerations on performance analysis and ethically significant biases. We used this part to evaluate the fairness of two DL models for LCS: a pulmonary nodule risk estimation model from Venkadesh et al. (2021), and Sybil, a lung cancer risk estimation model from Mikhael et al. (2023). We also evaluate the PanCan2b model from McWilliams et al. (2013), a multivariate logistic regressor popular in lung cancer screening protocols. We first examine whether our models have performance disparities between different groups in our datasets based on demographic characteristics. If any such biases have been found, we then assess prevalence disparities for clinical risk factors between subgroups, and examine performance when isolating for these confounders. We assess these biases according to the JustEFAB ethical framework for integrating machine learning in clinical practice (Mccradden et al., 2023), and briefly reflect on future research needed in the field of algorithmic fairness.

2. Methods

This study aims to evaluate the fairness of three risk estimation models for lung cancer screening on the NLST cohort. We performed a two-stage analysis, first investigating disparities in model performance between demographic subgroups, and then evaluating the fairness of these disparities based on confounding from lung cancer risk factors. The code for this analysis is publicly accessible online².

2.1 NLST Dataset

This retrospective study evaluated fairness using LDCT examinations from NLST participants (National Lung Screening Trial Research Team et al., 2011). NLST was a multi-center randomized controlled clinical trial which screened participants at 33 different centres in the USA between 2002 and 2007. In total, 53,454 participants were recruited, and 26,722 participants were randomly assigned to receive three annual screenings with low-dose chest CT. These participants were selected as high-risk on account of being between the ages of 55 and 74 years old and having smoked at least 30 pack-years of cigarettes by the start of the trial. NLST participants completed a wide-ranging questionnaire before screening, reporting demographic characteristics, smoking behavior, histories of work, diseases disease and previous cancers, and their family's history of lung cancer. Information regarding the status, type, diagnosis, and survival outcomes of lung cancer was also recorded during screening. This trial received approval from the institutional review boards from all 33 centers involved, and obtained informed consent from all participants. Permission to use the data for this study was obtained from the NLST through the National Cancer Institute Cancer Data Access System (approved Project ID: NLST-1268).

Both DL models were trained on subsets of NLST data (Venkadesh et al., 2021; Mikhael et al., 2023). While these models were trained on different NLST subsets, their training sets contain very similar demographic characteristics, shown in Tables 7 and 8 in the Appendix. These models were chosen because they were both trained using NLST data, this motivated us to focus our investigation on whether the cause of biases was likely related to disparities in the dataset (if models shared the same bias), or whether they likely stemmed from differences in the model training process (if one model exhibited a bias not observed in another model). We performed an internal validation of our models' biases using a subset of NLST data at the scan level, since Sybil does not return nodule-level risk estimates. For the Venkadesh21 model and PanCan2b, we employed the maximum malignancy score for a nodule as its score for a LDCT scan. Our internal validation subset included all scans from the dataset from Venkadesh et al. (2021), excluding any scans found in Sybil's training set. This, along with using purely predictions from validation folds from the Venkadesh21 model, ensured that no predictions are from the training data itself. After this selection, our validation set consisted of 5,911 scans from 3,492 participants to evaluate the Venkadesh21 model, Sybil, and PanCan2b. Demographic characteristics of this scan-level dataset are included in Table 1.

2. <https://github.com/DIAGNijmegen/bodyct-lung-malignancy-fairness>

Table 1: Demographic characteristics of the NLST validation set (n=5911 scans). HS = High School.

Characteristic	Subgroup	Malignant (n=581)	Benign (n=5330)	All Scans (n=5911)
Education Status	8th grade or less	9 (1.5)	102 (1.9)	111 (1.9)
	9th-11th grade	32 (5.5)	258 (4.8)	290 (4.9)
	Associate Degree	126 (21.7)	1175 (22.0)	1301 (22.0)
	Bachelors Degree	96 (16.5)	817 (15.3)	913 (15.4)
	Graduate School	76 (13.1)	778 (14.6)	854 (14.4)
	HS Graduate / GED	141 (24.3)	1338 (25.1)	1479 (25.0)
Race	Post-HS training	87 (15.0)	765 (14.4)	852 (14.4)
	Asian	6 (1.0)	66 (1.2)	72 (1.2)
	Black	28 (4.8)	160 (3.0)	188 (3.2)
	More than one race	6 (1.0)	59 (1.1)	65 (1.1)
	Native American	8 (1.4)	15 (0.3)	23 (0.4)
	Native Hawaiian	1 (0.2)	17 (0.3)	18 (0.3)
Ethnicity	White	530 (91.2)	4993 (93.7)	5523 (93.4)
	Hispanic/Latino	4 (0.7)	94 (1.8)	98 (1.7)
Sex	Not Hispanic/Latino	574 (98.8)	5205 (97.7)	5779 (97.8)
	Female	244 (42.0)	2226 (41.8)	2470 (41.8)
Age	Male	337 (58.0)	3104 (58.2)	3441 (58.2)
	Weight	175 (50)	180 (50)	180 (50)
Height	Median (IQR)	68 (6)	68 (6)	68 (6)
Body Mass Index	Median (IQR)	26 (4)	27 (6)	26 (6)
Age	Median (IQR)	64 (8)	62 (8)	62 (8)

2.2 Risk Estimation Models

We analyzed two deep learning risk estimation models in this study both trained on NLST (National Lung Screening Trial Research Team et al., 2011), along with the PanCan2b risk calculator trained on the PanCan cohort. We used the models as specified in their original publications (Venkadesh et al., 2021; Mikhael et al., 2023; McWilliams et al., 2013) and in relevant supplementary material, to prioritize understanding each model’s potential biases in their publicly-available state. All models return risk scores between 0.0 and 1.0. An overview of each model’s training dataset size, input type and output is in Table 2.

2.2.1 Venkadesh21

The first model we analyzed in this study was a malignancy risk estimation model for pulmonary nodules developed by Venkadesh et al. (2021). This model takes a LDCT scan and XYZ-coordinates of previously detected pulmonary nodules, annotated by an expert radiologist and two trained medical students. It then extracts a $50mm^3$ patch around the nodules and this 3D patch is subsequently processed by two deep learning models. The first model extracts features from nine 2D views of the nodule area using a ResNet50 CNN backbone and combines them with a fully-connected layer to extract a malignancy risk score. The second model extracts features from the 3D nodule volume using a 3D Inception-

v1 CNN and processes them using a linear layer to obtain a single risk score. The Venkadesh21 model was trained using 10-fold cross validation and the final score consisted of an average of the 20 resulting models. It was optimized using a cross entropy loss, comparing predictions to data from NLST regarding whether lung cancer was found. The final outputs are calibrated³ using a two-parameter logistic regression with Platt scaling.

This DL model demonstrated comparable performance to thoracic radiologists, and significantly outperformed PanCan2b, when examining area under the receiver operator characteristic curve (AUROC) when evaluated on an independent cohort of nodules from the Danish Lung Cancer Screening Trial (Wille et al., 2016). This algorithm is freely available online for research purposes⁴.

2.2.2 Sybil

Sybil is a deep learning model for estimating lung cancer risk for the next six years after a given full LDCT scan, developed by Mikhael et al. (2023). An LDCT image is passed through a ResNet3D encoder to obtain embeddings which are then passed through two separate layers. The first is a 3D max

3. <https://www.diagnijmegen.nl/software/nodule-malignancy-risk-calibration/>

4. <https://grand-challenge.org/algorithms/pulmonary-nodule-malignancy-prediction/>

Table 2: Overview of inputs and outputs for the models. N refers to the amount of data of the specified input type.

Model	Input Type	N (Train / Test)	Additional Information
Venkadesh21	50mm ³ Block Around Nodule in LDCT	16,077	— Trained with 10-fold cross-val.
Sybil	Full LDCT (+ training annotations)	26,182	13,121 Outputs scores for next 6 years.
PanCan2b	Nodule, Scan and Participant Characteristics	7,008	5,021 Trained on the PanCan trial.

pooling layer. The second is an attention-based pooling layer that identifies features from CT slices and regions most relevant to Sybil’s lung cancer risk predictions. The outputs of both of these layers are concatenated and ran through a hazard layer, which calculates cumulative probabilities of lung cancer risk over the six years after a LDCT. Sybil was trained five times with final predictions as the average of this ensemble, with three components to its loss function. The first is a cross entropy loss comparing Sybil’s predictions for each of the next six years with whether a diagnosis happened at that time, according to NLST. The other two components correspond to whether the attention aligned with any included information about the cancerous lung and the bounding box annotations. Finally, the outputs are calibrated using an isotonic regressor. Sybil performed well when evaluated on a NLST test set and screening datasets from two hospitals in the USA and Taiwan (Mikhael et al., 2023), and the model and code are available freely online⁵. We used the Year 1 scores from Sybil in our analysis, since this score was the most directly comparable to estimations of the other models, which aim to predict the current risk of lung cancer in an LDCT at baseline.

2.2.3 PanCan2b (Brock Model)

We also assessed the fairness of the Brock nodule malignancy risk estimation model developed by McWilliams et al. (2013), in particular its PanCan2b variation. This is a multivariate logistic regression model based on statistical analysis of lung cancer risk factors in a dataset from the Pan-Canadian Early Detection of Lung Cancer study (Pan-Can), containing 7,008 nodules from 2,537 participants. Factors included in this analysis are those available in the dataset which were known at the time to be associated with lung cancer, along with nodule characteristics that can be determined from an LDCT at the time of screening. From this analysis, McWilliams et al. (2013) developed a parsimonious model “PanCan1a” which significantly links female sex, larger nodules, and nodules in the upper lung with lung cancer risk ($p < 0.05$). They also developed a full model “PanCan2a” which added factors significant at $p < 0.25$: age, family history of LC, emphysema, nodule type, and the number of nodules per scan. Additional models including nodule spiculation were also developed (“PanCan1b” and

“PanCan2b”).

These models’ performances were validated on participants from a trial in British Columbia with AUROC scores above 0.90. They have subsequently been validated in various settings and have shown strong overall performance, with the full model achieving higher AUROC than the parsimonious model (Chen et al., 2025). The Brock model has been applied in the nodule management guideline for the International Lung Screening Trial (ILST) (Lim et al., 2020), with the PanCan2b full model with spiculation recommended by the British Thoracic Society for nodule management (Baldwin, 2016). In the ILST protocol, a PanCan2b malignancy risk score of 6% (0.06) or above is associated with a moderate malignancy risk, and a follow-up LDCT is recommended after 3 months, instead of an annual or biennial LDCT at lower risk levels (Lim et al., 2020).

2.3 JustEFAB Ethical Framework

For this study, we applied part of the *Justice, Equity, Fairness, and Anti-Bias* (JustEFAB) group fairness framework as proposed by Mccradden et al. (2023), which recognizes the sociotechnical character of AI systems and draws on principles of medical and research ethics, feminist philosophy of science, and theories of justice. Like many other ethical frameworks in AI fairness (Obermeyer et al., 2021; Richardson and Gilbert, 2021; Giovanola and Tiribelli, 2023), JustEFAB examines the entire lifecycle of AI models, though we believe its careful ethical consideration of the links between demographics and confounders is particularly relevant for LCS. From JustEFAB, we primarily focused on Stage 1A (Design and Development) and Stage 1B (Ethical Decision Making), primarily analyzing the fairness of the data used by the models and choices made during training. We were less concerned with bias in the NLST label annotations, since evaluating the NLST protocol for diagnosing lung cancer was out of scope for this study, so we therefore assumed the provided labels truly reflect lung cancer.

For this study, we adopted the definition of algorithmic bias as written in JustEFAB, referring to a performance disparity leading to disparate impacts for a demographic group. We primarily defined fairness as a lack of *ethically significant bias*, defined in JustEFAB as a performance disparity which would systematically have negative consequences for a demographic group’s treatment based on

5. <https://github.com/reginabarzilaygroup/Sybil.git>

their identity and not on clinical need (Mccradden et al., 2023). Within this context, we use the separation criteria for AI fairness as defined by Barocas et al. (2023) within the JustEFAB framing, controlling for clinical need by examining potential confounders. In this LCS context, we were primarily concerned with minimizing two negative outcomes: overestimation (false positives) and underestimation (false negatives) of lung cancer risk.

2.4 Stage 1: Subgroup Performance Analysis

Based on demographic characteristics from NLST, we split the validation cohort into separate subgroups, and evaluated the models' performance on each subgroup. Figure 1 displays the process for performing this analysis for one model on a single characteristic. For binary categories (such as sex and race), we compared performance directly between groups, while with numerical characteristics (i.e. age, weight, height), we split the cohort based on the median in the overall NLST dataset (see Table 1). We calculated body mass index (BMI) using the provided height and weight, and split the cohort based on the 25 kg/m^2 threshold between normal-weight and overweight people, as recognized by the World Health Organization (Organization, 2005). For education, we divided the cohort between those who received a high school diploma, GED, or higher, and those who had only received an education up to the 11th grade.

We evaluated overall performance by comparing the AUROC for each model between subgroups. Significance was determined with a two-tailed hypothesis test ($\alpha = 0.05$) from Hanley and McNeil (1982). This test between two independent populations accounts for class imbalance by directly considering the number of malignant and benign scans from each group in its calculation.

To examine underestimation and overestimation of lung cancer risk, we also compared model sensitivity and specificity between subgroups. This was conducted at three thresholds, set for each model based on the overall validation set: 90% overall sensitivity, 90% overall specificity, and the "moderate risk" threshold of 6% used for the Brock model, which is being applied in the ILST (Lim et al., 2020). Table 3 displays the thresholds on our NLST validation cohort. We collected 95% confidence intervals (CIs) for ROC curves, sensitivity and specificity using 1000 bootstraps. We evaluated a disparity in sensitivity and specificity as *substantial* when a model's CIs between subgroups do not intersect.

2.5 Stage 2: Fairness Assessment

If performance disparities between demographic subgroups for any model were discovered in Stage 1, our next step was to assess whether they are unfair, according to JustEFAB (Mccradden et al., 2023). This allowed us to analyze

Table 3: Thresholds used to evaluate model performance on NLST. All models are also evaluated on the Brock ILST 6% (0.06) moderate risk threshold (Lim et al., 2020).

	90% Sensitivity	90% Specificity
Venkadesh21	0.049	0.222
Sybil (Year 1)	0.003	0.058
PanCan2b	0.015	0.165

whether the disparities are the result of biases in the training data or the trained algorithm, or just due to inherent challenges in the task across different groups. We assessed fairness by examining disparities in the prevalence of potential clinical confounders between subgroups. These included nodule and LDCT characteristics, participants' smoking and work histories in fields relevant to lung cancer, and previous diagnosis of diseases and cancers. Between subgroups, we measured a prevalence disparity as the difference in the percentage of participants with a particular risk factor. Here, we also split numerical risk factors based on their median in the NLST dataset, except for the number of nodules in a LDCT (split into bins of 1 nodule and more than 1 nodule).

We evaluated performance disparities between subgroups for the 10 factors with the highest prevalence disparity between them. The process for each factor is detailed in Figure 1. We employed the same metrics as in Stage 1, with a particular focus on the metric(s) for which a bias was observed. For each risk factor, we examined the model's performance between demographic subgroups in two NLST subsets: 1) the scans in which the risk factor was present, and 2) the scans where this factor was *not* present. If the performance disparity from Stage 1 persisted in either subset, then the bias was determined to not be confounded by that factor. This persistence was based first on the p value between AUROC and the non-intersection of CIs for sensitivity and specificity, and second on the difference in the performance metrics between demographic subgroups. If the performance disparity was no longer significant and reduced for both subsets, then the factor may be a potential confounder. However, assessing fairness with JustEFAB requires a careful examination of clinical need: if a factor is linked to the demographic through selection bias and not biology (Jones et al., 2024), or not related to lung cancer risk, then it is deemed unfair (Mccradden et al., 2023).

3. Results

We first report the results of the subgroup performance analysis, highlighting demographic performance disparities identified for the models. Comprehensive results are provided in Tables 4 (AUROC), 5 (sensitivity) and 6 (specificity). For each demographic group where a performance disparity

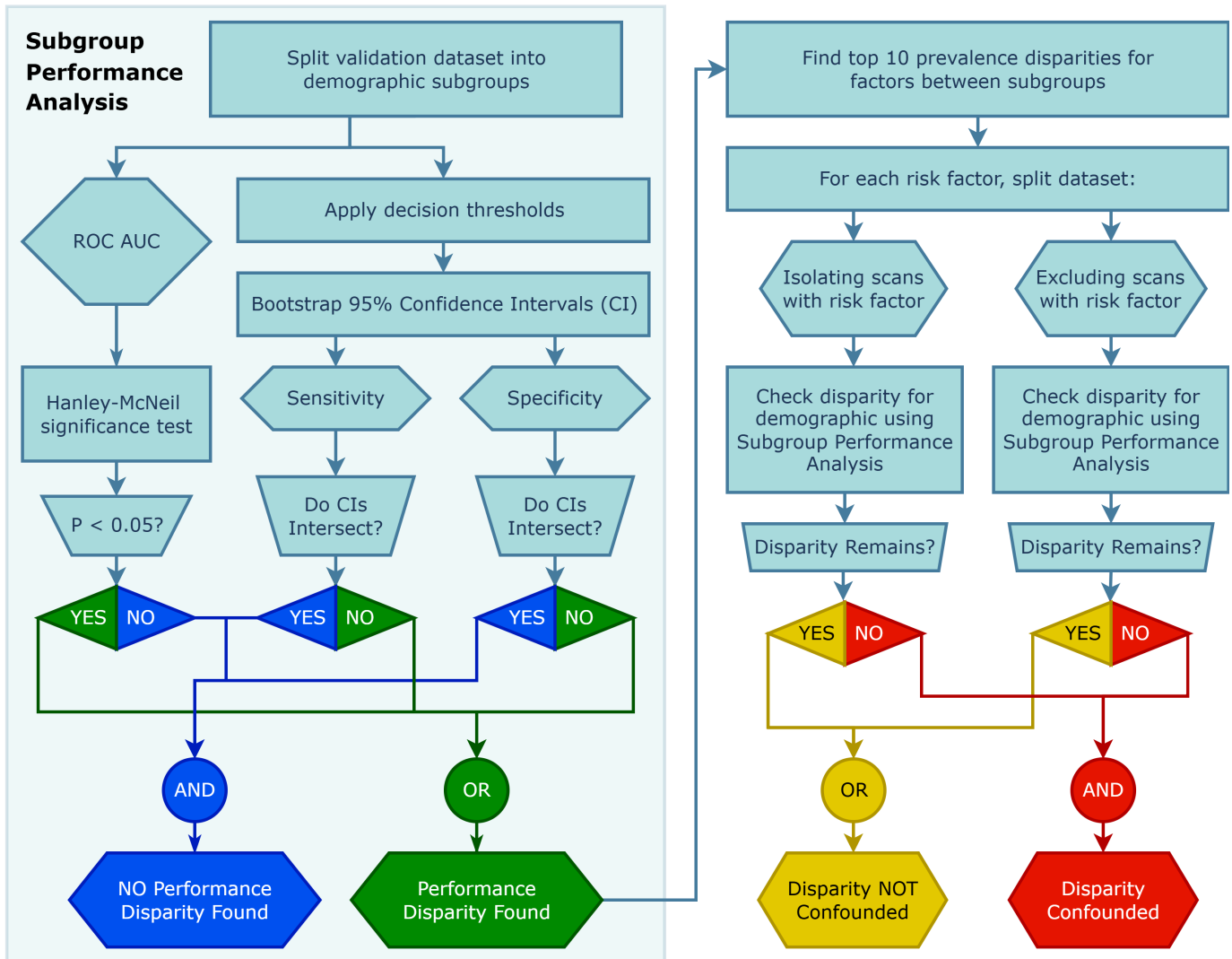


Figure 1: Flowchart of subgroup performance analysis (left) and fairness assessment (right) for a single model on a single demographic characteristic. Color coding indicates the decision paths to follow to reach a result (ex. disparity found).

was observed, we subsequently analyzed potential contributing risk factors. Specifically, we report the most prevalent clinical confounders and evaluate model performance when stratifying by or excluding these variables.

3.1 Subgroup Performance Analysis

Sybil demonstrated a statistically significant difference in performance by sex, achieving an AUROC of 0.88 (0.86, 0.90) for women and 0.81 (0.78, 0.84) for men ($p < .001$), as shown in Figure 2. Controlling for 90% specificity overall, Sybil showed a substantial difference of 0.13 in sensitivity between women (Sensitivity: 0.66 (0.60, 0.71)) and men (Sensitivity: 0.53 (0.48, 0.58)), as shown in Table 5. Controlling for 90% sensitivity, Sybil exhibited a 0.10 lower specificity for men (Specificity: 0.46 (0.44, 0.48)) than women (Specificity: 0.56 (0.54, 0.58)). The Venkadeswari model showed a 0.04 higher specificity for women at the Brock ILST threshold, though no other substantial sensi-

tivity and specificity disparities, and no significant AUROC disparity. Conversely, PanCan2b appeared to have slightly higher sensitivity for women than men, but substantially lower specificity across thresholds, up to 0.13 lower at a 90% sensitivity threshold (see Table 6).

In this study, Sybil performed non-significantly better for participants with a BMI of 25 kg/m^2 or above (AUROC: 0.86 (0.84, 0.88)) than those with a lower BMI (AUROC: 0.81 (0.78, 0.85), $p = 0.05$). PanCan2b performed significantly better for the higher-BMI subgroup (AUROC: 0.81 (0.79, 0.83)) than the lower-BMI subgroup (AUROC: 0.73 (0.70, 0.77), $p = 0.001$), as shown in Table 4. Considering the factors behind BMI, Sybil demonstrated a significant performance disparity between participants with a height shorter than 68 inches (AUROC: 0.87 (0.85, 0.89)) than with taller participants (AUROC: 0.80 (0.77, 0.83), $p < 0.001$), but had little to no performance disparity ($p = 0.82$) between participants weighing more or fewer than 180 pounds. All models appeared to have lower

Table 4: AUROC (with 95% confidence intervals) for models for demographic subgroups on NLST.

Attribute	Group	Venkadesh21		Sybil (Year 1)		PanCan2b	
		AUROC	p	AUROC	p	AUROC	p
Age	> 61	0.88 (0.86, 0.90)		0.84 (0.82, 0.86)		0.76 (0.74, 0.79)	
	≤ 61	0.90 (0.88, 0.92)	.14	0.85 (0.82, 0.88)	.67	0.81 (0.78, 0.83)	.05
BMI	≥ 25	0.90 (0.88, 0.91)		0.86 (0.84, 0.88)		0.81 (0.79, 0.83)	
	< 25	0.88 (0.85, 0.90)	.32	0.81 (0.78, 0.85)	.05	0.73 (0.70, 0.77)	.001
Education	≥ HS	0.89 (0.88, 0.91)		0.85 (0.83, 0.86)		0.78 (0.76, 0.80)	
	< HS	0.85 (0.78, 0.92)	.32	0.82 (0.75, 0.89)	.55	0.78 (0.71, 0.85)	.98
Height	≤ 68	0.89 (0.87, 0.91)		0.87 (0.85, 0.89)		0.79 (0.76, 0.81)	
	> 68	0.88 (0.86, 0.91)	.67	0.80 (0.77, 0.83)	< .001	0.78 (0.75, 0.80)	.71
Race	White	0.89 (0.88, 0.91)		0.84 (0.83, 0.86)		0.78 (0.76, 0.80)	
	Black	0.82 (0.74, 0.89)	.14	0.83 (0.74, 0.90)	.77	0.75 (0.65, 0.83)	.54
Sex	Male	0.89 (0.87, 0.91)		0.81 (0.78, 0.84)		0.79 (0.76, 0.81)	
	Female	0.89 (0.87, 0.91)	.92	0.88 (0.86, 0.90)	< .001	0.78 (0.75, 0.81)	.66
Weight	≤ 180	0.88 (0.87, 0.90)		0.84 (0.82, 0.87)		0.77 (0.74, 0.79)	
	> 180	0.89 (0.87, 0.91)	.65	0.84 (0.81, 0.87)	.82	0.80 (0.77, 0.82)	.13

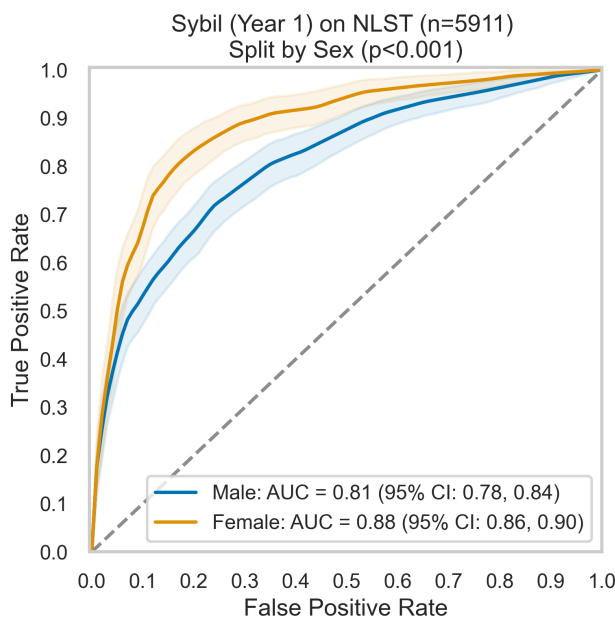


Figure 2: ROC curves (with 95% CIs) for Sybil (Year 1) for men and women on NLST (n=5911 scans).

specificity (and thus more false positives) with scans from participants with a lower BMI, as shown in Figure 3a.

The Venkadesh21 model exhibited non-significantly better performance with White participants (AUROC: 0.89 (0.88, 0.91)) than Black participants (AUROC: 0.82 (0.74, 0.89), $p = 0.14$). When applying thresholds, we observed that this model had a higher sensitivity for White participants, as shown in Figure 3b. In particular, the Venkadesh21 model had a substantial 0.30 difference in sensitivity for White participants (Sensitivity: 0.69 (0.65, 0.73)) than

Black participants (Sensitivity: 0.39 (0.23, 0.59)) when applying a threshold which would result in a 10% overall false positive rate (or 90% specificity) for this model. Even without a significant AUROC disparity, this disparity indicates that the Venkadesh21 model has disparate performance between racial subgroups (see Figure 1).

Finally, we observed higher false positive rates from all three models with NLST participants older than 61 years of age, and those who had not graduated high school or received further education. While we did not observe significant differences in AUROC or specificity between participants with lower and higher education, all models achieved substantially lower specificity for participants who had not graduated high school in the 90% sensitivity threshold (see Figure 3d). Between age groups, all models exhibited substantially lower specificity (0.07 lower for Venkadesh21 and 0.12 lower for the other models) for older participants when controlling sensitivity to 90%, as shown in Figure 3c.

3.2 Fairness Assessment

In this analysis, we examined whether the observed performance biases could be explained by differences in the prevalence of clinical risk factors. We investigated Sybil's performance disparity between men and women, the Venkadesh21 model's lower sensitivity for Black participants compared to White participants at a 90% specificity threshold, AUROC and specificity disparities observed in Sybil and PanCan2b between participants with a low and high BMI, and the disparate specificity for all models between participants who had and had not graduated high school. We did not separately assess confounders for Sybil's disparity between height-based subgroups, since it is directly a factor in BMI,

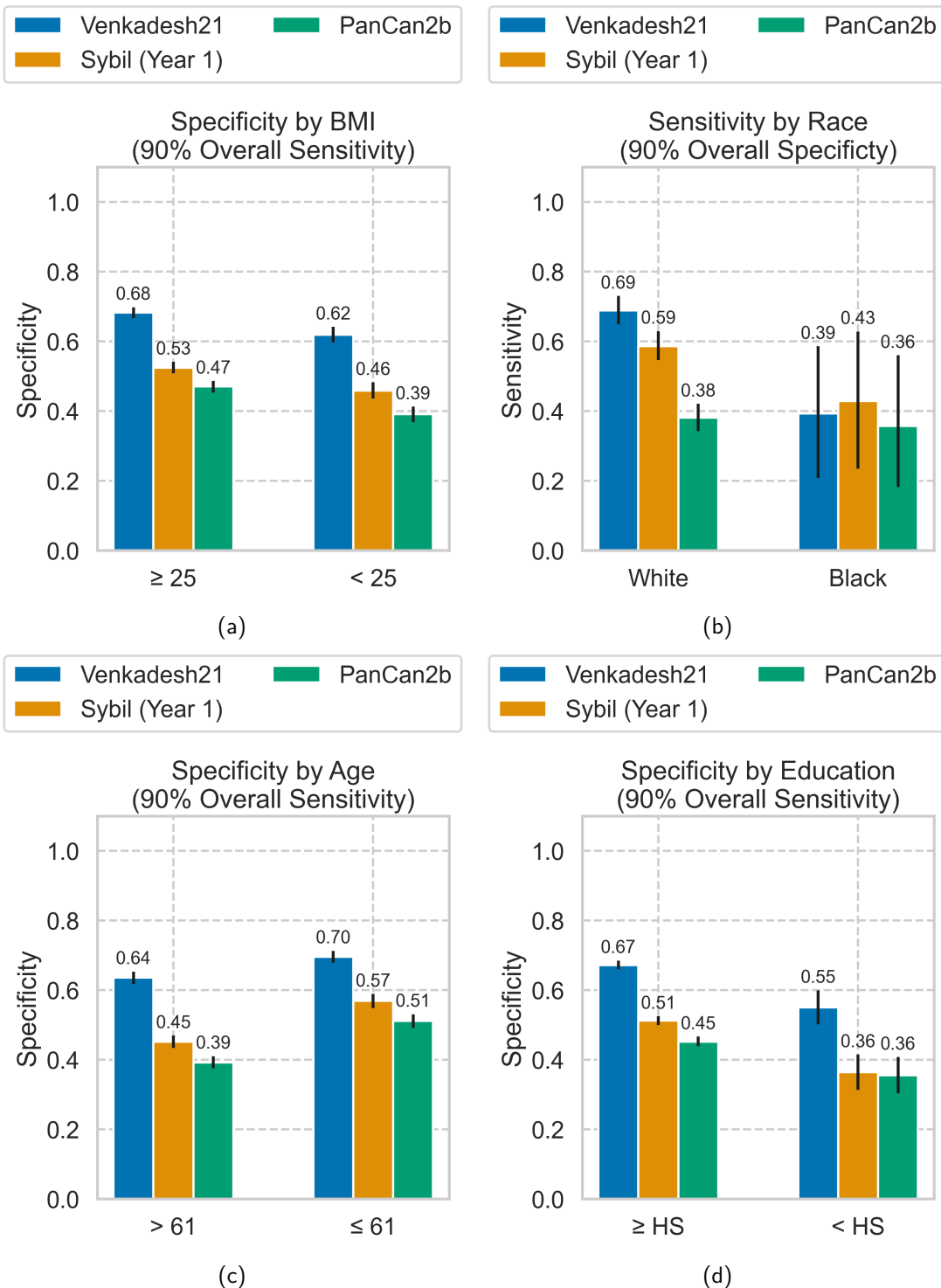


Figure 3: Selected sensitivity and specificity of models on specific thresholds on NLST (n=5911 scans).

and highly related to sex in the NLST cohort. We also did not assess potential confounding for the apparent overestimation of lung cancer risk in older LCS participants, as age is a clinically established risk factor for developing cancer (de Groot et al., 2018). Tables displaying comprehensive results are provided in the Appendix.

3.2.1 Disparity for Sybil Between Sexes

We first assess Sybil's disparity between sexes. Men in the NLST cohort were more likely to smoke pipes and cigars and work in a hazardous field for the lungs without a mask, while women were more likely to live with a smoker and have a previous pneumonia diagnosis. Table 9 (see Appendix) displays the 10 characteristics with the greatest prevalence differences between men and women. Men had higher

Table 5: Sensitivity (with 95% confidence intervals) for models for demographic subgroups on NLST. Single asterisk (*) = sensitivity of one subgroup is outside the CI of the other. Double asterisks (**) = CIs do not intersect.

Policy	Attribute	Group	Venkadesh21		Sybil (Year 1)		PanCan2b	
			Sensitivity	CI	Sensitivity	CI	Sensitivity	CI
90% Overall Sensitivity								
Age	> 61	0.90 (0.86, 0.93)		0.91 (0.88, 0.94)	0.92 (0.89, 0.95)			
	≤ 61	0.91 (0.87, 0.94)		0.90 (0.86, 0.94)	0.87 (0.82, 0.91)	*		
BMI	≥ 25	0.90 (0.87, 0.93)		0.92 (0.89, 0.94)	0.91 (0.88, 0.94)			
	< 25	0.90 (0.86, 0.94)		0.89 (0.84, 0.93)	0.88 (0.84, 0.92)			
Education	≥ HS	0.90 (0.87, 0.92)		0.91 (0.88, 0.93)	0.90 (0.88, 0.93)			
	< HS	0.88 (0.77, 0.97)		0.90 (0.80, 0.98)	0.88 (0.78, 0.97)			
Height	≤ 68	0.90 (0.87, 0.94)		0.92 (0.90, 0.95)	0.92 (0.89, 0.95)			
	> 68	0.90 (0.86, 0.93)		0.89 (0.85, 0.92)	0.88 (0.84, 0.92)	*		
Race	White	0.90 (0.88, 0.93)		0.91 (0.89, 0.93)	0.90 (0.87, 0.93)			
	Black	0.82 (0.67, 0.96)		0.86 (0.71, 0.97)	0.89 (0.75, 1.00)			
Sex	Male	0.90 (0.87, 0.93)		0.90 (0.86, 0.93)	0.88 (0.85, 0.92)			
	Female	0.90 (0.86, 0.93)		0.92 (0.89, 0.96)	0.92 (0.89, 0.95)	*		
Weight	≤ 180	0.91 (0.88, 0.94)		0.92 (0.89, 0.95)	0.91 (0.88, 0.94)			
	> 180	0.89 (0.85, 0.93)		0.89 (0.86, 0.93)	0.89 (0.85, 0.92)			
Age	> 61	0.70 (0.65, 0.75)		0.61 (0.56, 0.66)	0.40 (0.35, 0.44)			
	≤ 61	0.65 (0.58, 0.71)		0.53 (0.47, 0.60)	*	0.37 (0.32, 0.44)		
BMI	≥ 25	0.68 (0.63, 0.72)		0.58 (0.53, 0.62)	0.37 (0.33, 0.43)			
	< 25	0.69 (0.63, 0.75)		0.59 (0.52, 0.65)	0.41 (0.34, 0.48)			
Education	≥ HS	0.68 (0.64, 0.72)		0.59 (0.55, 0.63)	0.39 (0.35, 0.43)			
	< HS	0.68 (0.54, 0.82)		0.56 (0.41, 0.71)	0.41 (0.26, 0.57)			
Height	≤ 68	0.70 (0.65, 0.75)		0.63 (0.58, 0.68)	0.43 (0.38, 0.48)			
	> 68	0.66 (0.61, 0.71)		0.52 (0.47, 0.58)	*	0.34 (0.29, 0.40)	*	
Race	White	0.69 (0.65, 0.73)		0.59 (0.55, 0.63)	0.38 (0.34, 0.42)			
	Black	0.39 (0.21, 0.59)	**	0.43 (0.24, 0.63)	0.36 (0.18, 0.56)			
Sex	Male	0.66 (0.61, 0.71)		0.53 (0.48, 0.58)	0.33 (0.28, 0.38)			
	Female	0.71 (0.65, 0.76)		0.66 (0.60, 0.71)	**	0.47 (0.41, 0.53)	**	
Weight	≤ 180	0.69 (0.64, 0.74)		0.59 (0.54, 0.64)	0.42 (0.36, 0.47)			
	> 180	0.68 (0.62, 0.74)		0.57 (0.51, 0.63)	0.35 (0.29, 0.41)	*		
Age	> 61	0.88 (0.84, 0.91)		0.61 (0.56, 0.66)	0.72 (0.66, 0.76)			
	≤ 61	0.89 (0.85, 0.93)		0.53 (0.47, 0.60)	*	0.67 (0.61, 0.73)		
BMI	≥ 25	0.89 (0.86, 0.92)		0.58 (0.53, 0.62)	0.70 (0.65, 0.75)			
	< 25	0.88 (0.82, 0.92)		0.59 (0.52, 0.65)	0.69 (0.63, 0.76)			
Education	≥ HS	0.88 (0.85, 0.91)		0.59 (0.55, 0.63)	0.69 (0.65, 0.73)			
	< HS	0.88 (0.77, 0.97)		0.56 (0.41, 0.71)	0.80 (0.68, 0.92)			
Height	≤ 68	0.89 (0.85, 0.92)		0.63 (0.58, 0.68)	0.72 (0.67, 0.77)			
	> 68	0.88 (0.84, 0.91)		0.52 (0.47, 0.58)	*	0.68 (0.62, 0.73)		
Race	White	0.89 (0.86, 0.91)		0.59 (0.55, 0.63)	0.69 (0.65, 0.73)			
	Black	0.75 (0.59, 0.91)		0.43 (0.24, 0.63)	0.68 (0.50, 0.85)			
Sex	Male	0.88 (0.84, 0.92)		0.53 (0.48, 0.58)	0.68 (0.62, 0.72)			
	Female	0.89 (0.85, 0.92)		0.66 (0.60, 0.71)	**	0.73 (0.68, 0.78)		
Weight	≤ 180	0.88 (0.84, 0.91)		0.59 (0.54, 0.64)	0.70 (0.65, 0.75)			
	> 180	0.89 (0.85, 0.92)		0.57 (0.51, 0.63)	0.69 (0.64, 0.75)			
Brock NLST (6%)								

smoking rates in NLST, with a median of 55 pack-years (IQR: 35) compared to 46 pack-years (IQR: 22) for women, though with similar rates of lung cancer (10% for both, as seen in Table 1). Male participants' median weight was 35

pounds heavier (and median height 7 inches taller) than that of women, but median BMIs were similar. For almost all of these factors, Sybil's AUROC disparity between men and women persisted when isolating for (or

Table 6: Specificity (with 95% confidence intervals) for models for demographic subgroups on NLST. Single asterisk (*) = specificity of one subgroup is outside the CI of the other. Double asterisks (**) = CIs do not intersect.

Policy	Attribute	Group	Venkadesh21		Sybil (Year 1)		PanCan2b	
			Specificity	CI	Specificity	CI	Specificity	CI
90% Overall Sensitivity	Age	> 61	0.64 (0.62, 0.65)		0.45 (0.43, 0.47)		0.39 (0.38, 0.41)	
		≤ 61	0.70 (0.68, 0.71)	**	0.57 (0.55, 0.59)	**	0.51 (0.49, 0.53)	**
	BMI	≥ 25	0.68 (0.67, 0.70)		0.53 (0.51, 0.54)		0.47 (0.45, 0.49)	
		< 25	0.62 (0.60, 0.64)	**	0.46 (0.44, 0.48)	**	0.39 (0.37, 0.41)	**
	Education	≥ HS	0.67 (0.66, 0.69)		0.51 (0.50, 0.53)		0.45 (0.44, 0.47)	
		< HS	0.55 (0.50, 0.60)	**	0.36 (0.31, 0.41)	**	0.36 (0.30, 0.41)	**
	Height	≤ 68	0.68 (0.66, 0.70)		0.55 (0.53, 0.57)		0.41 (0.39, 0.43)	
		> 68	0.64 (0.63, 0.66)	*	0.45 (0.43, 0.47)	**	0.48 (0.46, 0.50)	**
	Race	White	0.66 (0.65, 0.67)		0.50 (0.49, 0.51)		0.45 (0.43, 0.46)	
		Black	0.73 (0.66, 0.80)		0.59 (0.52, 0.66)	**	0.37 (0.29, 0.44)	*
90% Overall Specificity	Sex	Male	0.65 (0.63, 0.66)		0.46 (0.45, 0.48)		0.50 (0.48, 0.52)	
		Female	0.68 (0.66, 0.70)	*	0.56 (0.54, 0.58)	**	0.37 (0.35, 0.39)	**
	Weight	≤ 180	0.65 (0.63, 0.67)		0.49 (0.47, 0.51)		0.40 (0.38, 0.42)	
		> 180	0.68 (0.66, 0.69)	*	0.51 (0.49, 0.53)		0.49 (0.47, 0.51)	**
	Age	> 61	0.88 (0.87, 0.89)		0.89 (0.88, 0.90)		0.88 (0.86, 0.89)	
		≤ 61	0.92 (0.91, 0.93)	**	0.92 (0.91, 0.93)	**	0.93 (0.92, 0.94)	**
	BMI	≥ 25	0.91 (0.90, 0.92)		0.91 (0.90, 0.92)		0.92 (0.91, 0.92)	
		< 25	0.87 (0.86, 0.89)	**	0.89 (0.87, 0.90)	**	0.87 (0.85, 0.88)	**
	Education	≥ HS	0.90 (0.89, 0.91)		0.90 (0.90, 0.91)		0.90 (0.89, 0.91)	
		< HS	0.86 (0.83, 0.90)	*	0.89 (0.86, 0.92)		0.88 (0.84, 0.91)	
Brock NLST (6%)	Height	≤ 68	0.90 (0.89, 0.91)		0.90 (0.89, 0.92)		0.90 (0.88, 0.91)	
		> 68	0.90 (0.89, 0.92)		0.90 (0.89, 0.91)		0.91 (0.90, 0.92)	
	Race	White	0.90 (0.89, 0.91)		0.90 (0.90, 0.91)		0.90 (0.89, 0.91)	
		Black	0.93 (0.89, 0.97)		0.92 (0.88, 0.96)		0.88 (0.83, 0.93)	
	Sex	Male	0.90 (0.89, 0.91)		0.90 (0.89, 0.91)		0.91 (0.90, 0.92)	
		Female	0.90 (0.88, 0.91)		0.90 (0.89, 0.91)		0.88 (0.87, 0.89)	**
	Weight	≤ 180	0.89 (0.88, 0.90)		0.89 (0.88, 0.91)		0.88 (0.87, 0.89)	
		> 180	0.91 (0.90, 0.92)	**	0.91 (0.90, 0.92)	*	0.92 (0.91, 0.93)	**
	Age	> 61	0.67 (0.65, 0.69)		0.89 (0.88, 0.90)		0.69 (0.68, 0.71)	
		≤ 61	0.73 (0.71, 0.75)	**	0.92 (0.91, 0.93)	**	0.79 (0.77, 0.81)	**
Brock NLST (6%)	BMI	≥ 25	0.72 (0.70, 0.73)		0.91 (0.90, 0.92)		0.76 (0.75, 0.77)	
		< 25	0.66 (0.63, 0.68)	**	0.89 (0.87, 0.90)	**	0.68 (0.66, 0.71)	**
	Education	≥ HS	0.71 (0.69, 0.72)		0.90 (0.90, 0.91)		0.74 (0.73, 0.75)	
		< HS	0.59 (0.55, 0.64)	**	0.89 (0.86, 0.92)		0.69 (0.64, 0.73)	*
	Height	≤ 68	0.71 (0.70, 0.73)		0.90 (0.89, 0.92)		0.72 (0.70, 0.73)	
		> 68	0.68 (0.66, 0.69)	**	0.90 (0.89, 0.91)		0.76 (0.74, 0.77)	**
	Race	White	0.69 (0.68, 0.71)		0.90 (0.90, 0.91)		0.74 (0.72, 0.75)	
		Black	0.76 (0.68, 0.82)		0.92 (0.88, 0.96)		0.68 (0.60, 0.75)	
	Sex	Male	0.68 (0.66, 0.70)		0.90 (0.89, 0.91)		0.77 (0.76, 0.79)	
		Female	0.72 (0.70, 0.74)	**	0.90 (0.89, 0.91)		0.69 (0.67, 0.71)	**
	Weight	≤ 180	0.69 (0.67, 0.70)		0.89 (0.88, 0.91)		0.69 (0.68, 0.71)	
		> 180	0.71 (0.69, 0.72)	*	0.91 (0.90, 0.92)	*	0.78 (0.76, 0.80)	**

excluding) any single condition, as shown in Table 9 in the Appendix. As an example, men had a 34% rate of working in a dangerous field without a mask, while women only had a 13% rate of doing so. Isolating for only participants who

worked without a mask, men (109 malignant scans, 1075 benign scans) and women (30 malignant scans, 290 benign scans) both had an AUROC of 0.79 ($p = 0.92$), as shown in Figure 4. However, for participants without this work history,

Sybil still performed significantly better for women (AUROC: 0.89 (0.87, 0.91)) than for men (AUROC: 0.82 (0.79, 0.85), $p < 0.001$). This indicates that working without a mask did not confound Sybil's sex bias, since the disparity remained when excluding for working without a mask (see Figure 1). Conversely, the AUROC disparity between men and women was no longer significant when splitting the NLST cohort based on height. While there was still a 0.04 increase in AUROC from men to women, the difference was not significant for participants taller than 68 inches ($p = 0.63$) or for shorter participants ($p = 0.17$). This was also the factor with the greatest prevalence disparity between men and women, as 76% of men in NLST have a height greater than 68 inches, while this is the case for only 6% of women.

We also examined the impact of these factors on explaining the substantial disparity between sexes in sensitivity (at 90% specificity) and specificity (at 90% sensitivity). Examining these metrics revealed that Sybil still maintained performance disparities between men and women, even when isolating for potential confounders (see Table 10 in the Appendix). For each of these characteristics, Sybil's sensitivity and specificity was substantially better for women, with almost no CIs intersecting between sexes for any comparisons. Sybil demonstrated 0.08 better sensitivity for taller women than taller men and 0.11 greater sensitivity for shorter women than shorter men, with CIs intersecting between sexes. However, while the specificity for taller men and women were the same, shorter men tended to receive a substantially higher false positive rate than shorter women, with a gap of 0.08 and non-intersecting CIs.

3.2.2 Racial Disparity for Venkadesh21

With race, we focused on investigating the Venkadesh21 model's substantial sensitivity disparity between White and Black participants at 90% specificity, along with its non-significant AUROC disparity. White participants accounted for 93% of the NLST cohort, while Black participants accounted for only 3% of the data. Despite White participants having higher smoking rates (with medians of 51 pack-years and 25 average cigarettes per day) in NLST than Black participants (with medians of 43 pack-years and 20 average cigarettes per day), Black participants had a higher rate of lung cancer in the NLST cohort (15%) than White participants (10%). Black participants had higher rates of being current smokers (70%) instead of former smokers than White participants (50%), and had a previous hypertension diagnosis at a much higher rate (54%) than White participants (33%), as shown in Table 11 in the Appendix.

Investigating the impact of these confounders revealed that the Venkadesh21 model still exhibited (non-significantly) worse AUROC scores (see Table 11 in the Appendix) and substantially lower sensitivity (see Table 12 in the Appendix)

for Black participants. As an example, we investigated if the greater hypertension prevalence in Black participants confounded the Venkadesh21 model's reduced performance. When plotting ROC curves for participants without hypertension, we observed similar performance for Black participants (AUROC: 0.93, (0.87, 0.98)) than White participants (AUROC: 0.90 (0.89, 0.92), $p = 0.60$). However, we did observe an AUROC performance difference between White participants with hypertension (196 malignant scans, 1617 benign scans, AUROC: 0.87 (0.84, 0.90)) and Black participants with hypertension (16 malignant scans, 86 benign scans, AUROC: 0.73 (0.61, 0.85), $p = 0.04$), as shown in Figure 5. The sensitivity disparity, shown in Table 12 (see Appendix), also remained substantial between White participants with a hypertension diagnosis (Sensitivity: 0.65 (0.59, 0.72)) and Black participants with a hypertension diagnosis (Sensitivity: 0.19 (0.00, 0.40)). This indicates that a prevalence disparity for hypertension did not confound lower sensitivity for Black participants, as the Venkadesh21 model still showed disparate performance when isolating for participants diagnosed with this condition.

3.2.3 Body Mass Index Disparity

We also investigated further the lower AUROC and higher false positive rates for participants with a lower body mass index from our models, in particular Sybil's Year 1 risk score. Participants with a lower BMI in NLST were more likely to be current (and not former) smokers, were more likely to be pipe smokers, and had smoked more cigarettes per day than high BMI participants, but had similar pack-years, as detailed in Table 13 in the Appendix. Lower-BMI participants were more likely to have emphysema in a LDCT (47% compared to 32% for high-BMI participants) or be previously diagnosed with it, while high-BMI participants were more likely to have a diabetes or hypertension diagnosis.

Disparities persisted for most characteristics between high and low BMI participants. However, emphysema in the LDCT may have confounded Sybil's AUROC and specificity disparities, since isolating and excluding this factor resulted in reduced disparities between subgroups. Figure 6 shows that for low-BMI participants with emphysema in their scans (103 malignant, 789 benign), Sybil's AUROC was 0.78 (0.73, 0.83), close to that for high-BMI participants (161 malignant scans, 1103 benign scans, AUROC: 0.81 (0.77, 0.85), $p = 0.44$). Sybil exhibited similar performance for participants without emphysema. The specificity disparity was also smaller when isolating for emphysema (see Table 14 in the Appendix). Sybil's lower performance for low-BMI participants aligned with its significantly worse ($p < 0.001$) performance with emphysema (see Figure 7 in the Appendix).

However, it should be noted that the PanCan2b model,

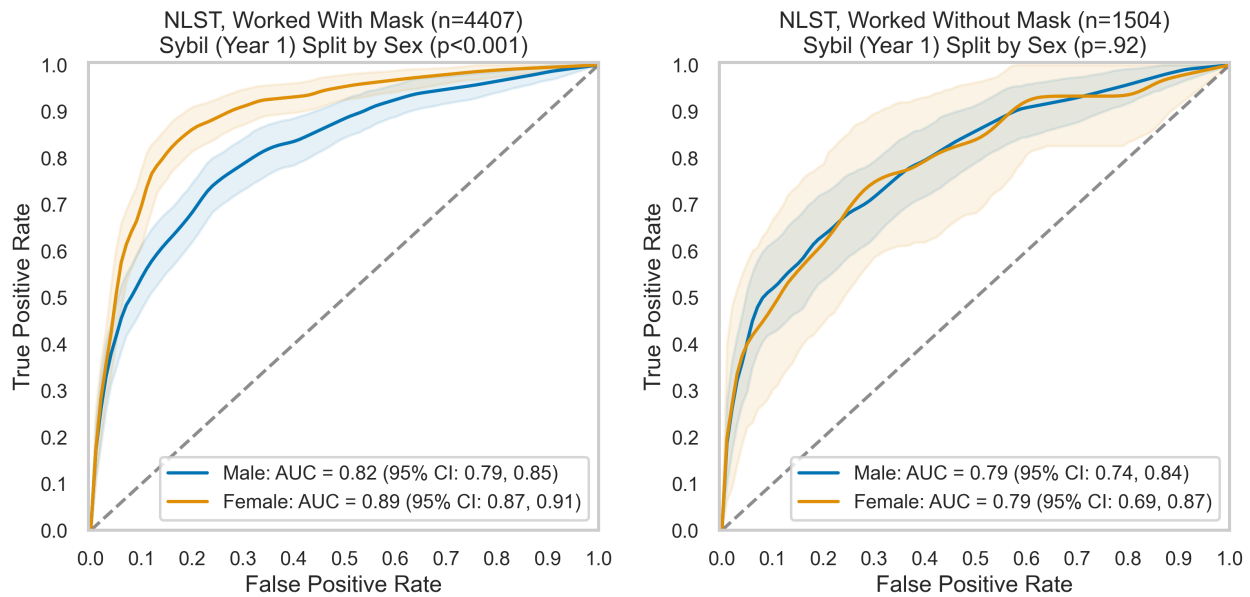


Figure 4: ROC curves (with 95% CIs) for Sybil (Year 1) between men and women when isolating for a self-reported work history of working in a dangerous occupation for the lungs with or without a mask.

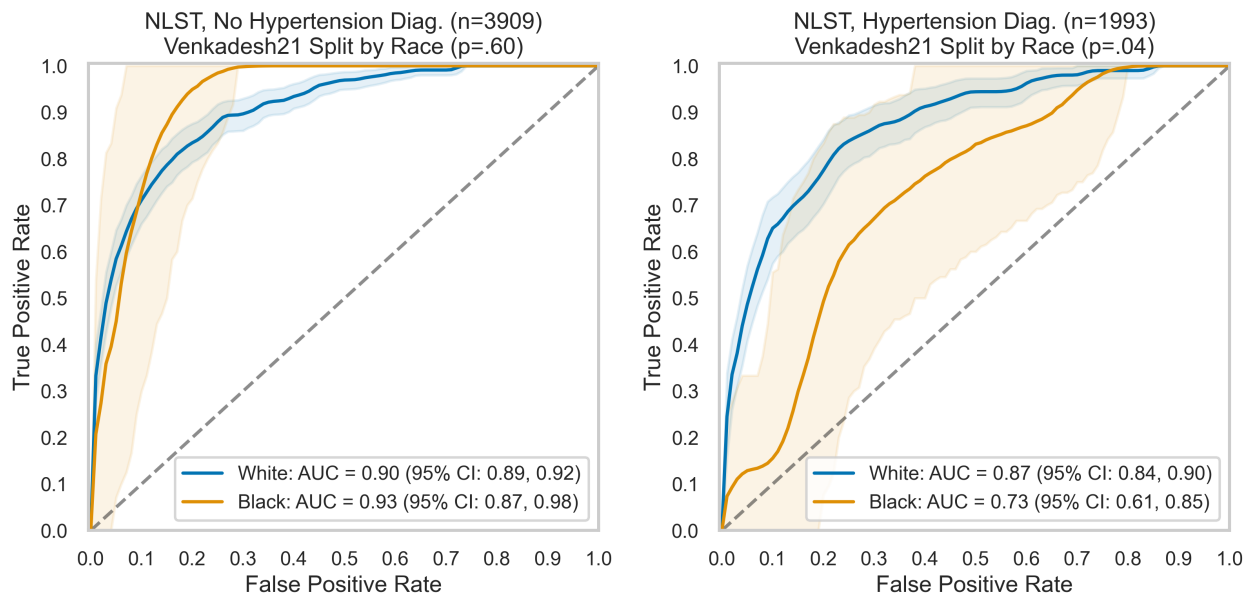


Figure 5: ROC curves (with 95% CIs) for Venkadesh21 between racial groups when isolating for a hypertension diagnosis.

which showed significant performance disparities against lower-BMI participants, did not appear to be confounded by any of these prevalence disparities. When inspecting ROC curves, PanCan2b appeared to retain significant AUROC disparities based on BMI when isolating or excluding these confounders, as shown in Table 15. For participants with emphysema, participants with lower BMI had an AUROC of 0.68 (0.62, 0.73), while higher-BMI participants had an AUROC of 0.80 (0.76, 0.83) ($p < 0.001$).

3.2.4 High School Graduation Disparity

Here, we further assessed the substantially lower specificity from all three models on participants who reported education levels lower than that of high school graduates. Examining the prevalence of risk factors between this subgroup and other participants (see Table 16 in the Appendix) revealed key disparities in age, work, and smoking. Non-graduates in NLST appeared to be older than graduates (with 70% above 61 years old, compared to 55% of graduates), but had started smoking earlier, perhaps explaining

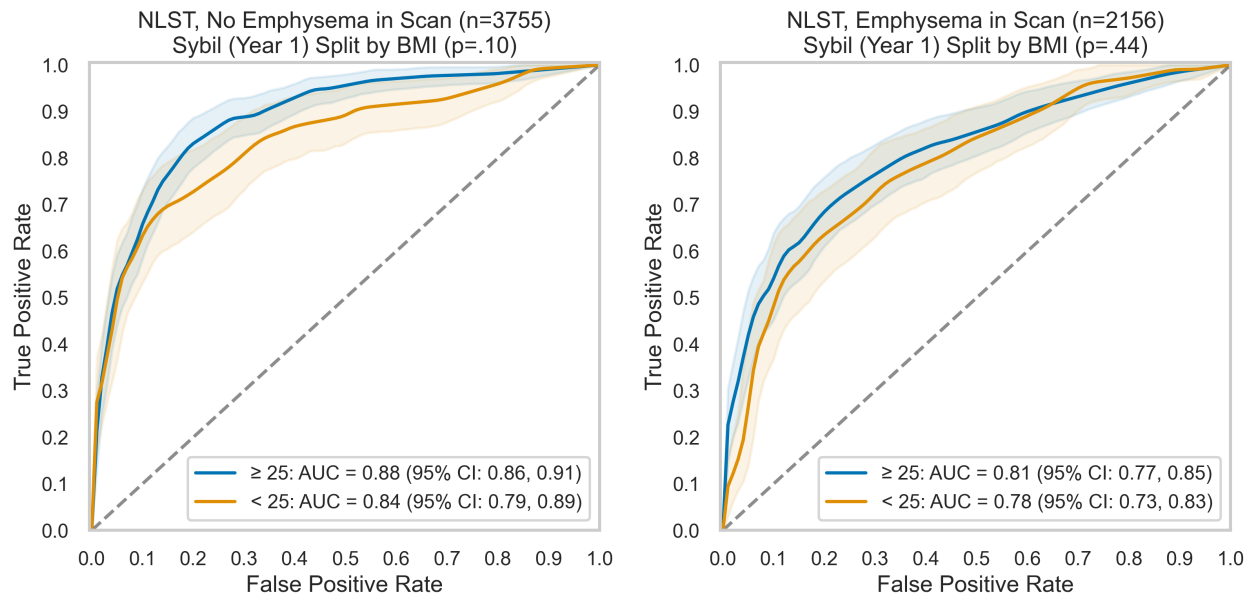


Figure 6: ROC curves (with 95% CIs) for Sybil (Year 1) between BMI groups when isolating for emphysema.

their greater pack-years, years of smoking, and likelihood of still smoking. They were also far more likely to work in welding and with a smoker, but less likely to work without a mask. Also, 71% of them had nodules with a diameter of 6mm or larger (compared to 62% of graduates).

When isolating and excluding these factors, Venkadesh21 and Sybil continued to exhibit substantially more false positives for non-graduates (see Tables 17 and 18 in the Appendix). However, PanCan2b's specificity disparity appeared to be confounded when splitting by age and nodule diameter, which can be seen in Table 19 in the Appendix. When isolating participants older than 61 years old, PanCan2b had a specificity of 0.40 (0.38, 0.42) for high school graduates and 0.33 (0.27, 0.39) for non-graduates, with slightly intersecting CIs. This was repeated for younger participants, indicating that age confounded this disparity for PanCan2b. For participants with nodules more than 6mm wide, PanCan2b achieved similar scores for graduates (specificity: 0.15 (0.14, 0.16)) and non-graduates (specificity: 0.11 (0.08, 0.15)). PanCan2b's disparity also did not persist for high school graduates and non-graduates with smaller nodules, demonstrating that PanCan2b's disparate specificity between these subgroups was confounded by nodule diameter as well as participant age.

4. Discussion

This study evaluated the fairness of three lung cancer risk estimation models through performance metrics, controlling for the impact of potential clinical confounders. We found four performance disparities that cannot always be explained by clinical risk factors, so we conclude that these

disparities are unfair and potentially caused by biases in the algorithms or training data. First, we observed that the Sybil full-lung cancer risk model (Mikhael et al., 2023) had overall lower performance for men, unrelated to prevalence disparities of potential clinical confounders. Second, the Venkadesh21 nodule risk estimation model (Venkadesh et al., 2021) exhibited lower sensitivity for Black Americans compared to White Americans at an operating point of 90% specificity, which was also not found to be influenced by prevalence disparities. Third, all models appeared to have lower specificity for participants with a lower body mass index, though for Sybil, this appears confounded by the prevalence of emphysema in an LDCT. Fourth, all models exhibited more false positives for participants who had not graduated high school, though PanCan2b's disparity was confounded by nodule diameter and age. In uncovering performance biases and investigating their fairness, this analysis aims to be a step towards further research into evaluation and mitigation of problematic AI biases, as well as discussions about the fairness of diagnostic AI systems.

4.1 Bias Between Sexes

This study uncovered a significant performance bias in Sybil between men and women in the NLST cohort across operating points. If deployed with a clinically relevant threshold such as 90% sensitivity or 90% specificity, Sybil's predictions would have had higher rates of overestimation and underestimation of lung cancer risk respectively for men than for women. This result differs from other studies which found no AUROC disparities between men and women in Sybil's Year 1 score in the NLST test set from Mikhael et al.

(2023) or from two American hospital screening datasets (Simon et al., 2023). This finding may be important since it highlights the potential for an AI model to exhibit different biases when deployed to different screening populations.

Even though Sybil was trained and evaluated on a 58% male dataset, it appeared to have better performance for women. This is contrary to the assumptions often made in AI fairness research, where a class imbalance in data is assumed to lead to lesser performance in the underrepresented subgroup. This raised questions about the cause of these performance disparities, including whether it was related to differences in potential clinical confounders between sexes. In the NLST data, both sexes had equal rates of lung cancer diagnosis, though men tended to be taller and heavier than women, had greater rates of smoking, and were more likely to work in dangerous fields without proper respiratory protection. This reflects clinical findings in sex disparities in smoking rates (Donington and Colson, 2011) and exposure to carcinogens (Kreuzer et al., 2000). However, Sybil's sex disparity persisted in the NLST cohort when isolating for (or excluding) any of these characteristics (including BMI and weight), with the exception of height. When comparing men and women of similar height, Sybil still achieved a higher AUROC for women, but this difference was reduced and not statistically significant. The disparity in sensitivity also became less substantial, though there remained an overestimation bias for shorter men compared to shorter women. While height showed a small effect in this analysis, it is not a clinical confounder of Sybil's sex bias, because there is no strong link between height and lung cancer risk (Abe et al., 2021; Le et al., 2024).

Since Sybil's disparate performance for men has not been shown to be linked to potential confounders, we determine that its performance disparity is unfair, according to JustEFAB. Depending on the performance threshold applied, using Sybil's risk estimations could lead to greater false negatives or false positives for men in LCS. Sybil's bias in sex (and also height) may potentially be related to shortcut learning, since it has been shown that Sybil could accurately predict sex, height and weight from a LDCT (Mikhael et al., 2023). Conversely, the Venkadesh21 nodule-only risk estimation model performed equally for both men and women across cohorts, indicating that examining only nodules may help to prevent a bias between sexes in lung cancer risk estimation.

This finding highlights the need for further discussion on the relationship between sex and lung cancer. While many studies have shown a link between the two, the biological connection between the two is unclear and a topic of ongoing research (Donington and Colson, 2011; Gasperino, 2011; May et al., 2023). As a result, some have argued that sex is an independent risk factor in LCS (Nakamura et al., 2011; Gasperino, 2011; Donington and

Colson, 2011). Moreover, some studies have found greater lung cancer survival rates for women in clinical settings (Nakamura et al., 2011) and LCS trials (de Koning et al., 2020; Pinsky et al., 2013). Sex is explicitly included in all four malignancy risk calculators in the Brock model, since it showed a significant relationship with lung cancer in the PanCan cohort (McWilliams et al., 2013). However, it should be noted that in our study's validation set, PanCan2b yielded greater sensitivity for women, though with more false positives. This may have resulted from the coefficient attributed to sex in its logistic regression model ($\beta = 0.6011$), which systematically gives women a higher score than men when controlling for other PanCan2b factors.

4.2 Bias Between Racial Groups

We observed in our experiments that the Venkadesh21 model exhibited lower sensitivity with Black American participants than White American participants. We did not observe such racial disparities in PanCan2b and Sybil's performance. The Sybil Year 1 score's lack of a racial performance disparity does not fully align with AUROC scores from previous NLST analysis by (Mikhael et al., 2023), though the previous analysis may be limited by the only 5 LDCTs with a lung cancer diagnosis from Black American participants in its testing set. When controlling for potential confounders such as hypertension and smoking status, we found that Venkadesh21's sensitivity disparity persisted. Therefore, due to a lack of explanation by potential confounders, we believe the Venkadesh21 model exhibited an unfair lower performance in Black American participants, underestimating their lung cancer risk. Considering that this model only examined nodules, we additionally investigated whether there were any differences in nodule types and size between Black and White participants. However, we did not observe any conclusive differences in nodule prevalence between these racial groups, due to the small number of samples from Black participants.

The racial bias present in this model may represent an example of health data poverty, where an underrepresented population is unable to benefit from new health technology due to insufficient data (Ibrahim et al., 2021). Black American participants made up only 3% of the NLST cohort, though with a higher rate of lung cancer while also reporting lower smoking rates than White participants. This was likely a result of screening criteria which may have missed potential Black participants for NLST (Aredo et al., 2022). Recent studies have shown that the median smoking rate for Black Americans with lung cancer fell below this threshold, meaning the 30-pack-year requirement for inclusion in NLST would miss the majority of lung cancer cases in this group, leading to lower sensitivity (Aredo et al., 2022). Overall, a lack of sufficiently diverse data for training the Venkadesh21

model likely led it to perpetuate a lower sensitivity for Black American participants in LCS.

4.3 Bias Relating to Body Mass Index

In our study, the Sybil Year 1 score also demonstrated a non-significantly worse AUROC for NLST participants with a BMI below 25 kg/m^2 compared to those with a higher BMI, while PanCan2b performed significantly worse. However, all models had lower specificity for lower-BMI participants, with non-intersecting confidence intervals across all three clinical thresholds. This indicates lower specificity for lower-BMI participants and potentially more false positive recommendations for this group. Both in NLST and in multiple clinical studies, lower BMI was linked with higher lung cancer risk, even when controlling for smoking factors and emphysema (Abe et al., 2021; Smith et al., 2012; El-Zein et al., 2013). We observed that disparities in specificity and AUROC from Sybil remain when controlling for smoking factors, indicating a lack of confounding.

However, our results showed that emphysema may have confounded Sybil's bias against lower-BMI participants, as the performance disparity reduced when isolating for participants with and without emphysema in the scan. Participants with a BMI below 25 kg/m^2 were more likely to have emphysema in the NLST cohort, which aligns with findings from another study which observed higher severity of emphysema for participants within this subgroup, though a causal relationship between obesity and emphysema is unknown (Gu et al., 2015). Emphysema is also a known risk factor for lung cancer and is already included in the PanCan2b model (McWilliams et al., 2013). However, this model's disparity against lower-BMI participants did not appear to be confounded by emphysema or other factors based on prevalence disparities.

From our analysis, the included models had similar sensitivity for participants regardless of their body mass index, though with more false positives for the population more at risk for lung cancer. Since this performance disparity was linked to the higher rates of lung cancer and emphysema in lower-BMI participants, the bias may be considered less ethically significant according to JustEFAB.

4.4 Bias Relating to High School Graduation

Education, along with income (which is not included in NLST) often forms a key component of a person's socioeconomic status (SES), so disparate behavior against those with lower education can indicate biases based on SES. In our study, all three models demonstrated substantially lower specificity for NLST participants who had reported education levels lower than a high school diploma or a GED than participants with this or a higher education level, at a 90% sensitivity threshold. This mirrors clinical studies

which found higher false positive rates for participants with lower SES (Castro et al., 2021), and lower lung cancer survival rates for communities with lower rates of people with a high school diploma (Erhunmwunsee et al., 2012). The models in our study did not appear to have significant AUROC disparities between these two subgroups, or substantial differences in sensitivity.

In our NLST validation cohort, non-graduates appeared to be older than high school graduates, with longer and more intense histories of smoking, reflecting similar findings from clinical studies (de Groot et al., 2018). They were also more likely to work in welding, work with smokers, and have larger pulmonary nodules (perhaps as a result). However, the Venkadesh21 and Sybil models' specificity disparities did not appear to be confounded by any of these factors. Therefore, according to JustEFAB, these two models' higher false positive rates for non-graduates appears to be unfair.

PanCan2b's disparity was confounded by nodule diameter, which is a known risk factor included in this model, having a positive nonlinear relationship with lung cancer in PanCan2b (McWilliams et al., 2013). Given that non-graduates in our NLST cohort are more likely to have larger nodules, this confounding appears fair according to JustEFAB. Its performance was also confounded by age, which is also factored in the model, with each additional year of a participant's age has a positive impact on the score ($\beta = 0.0287$) (McWilliams et al., 2013). With age being a known lung cancer risk factor as well, this would appear as a fair disparity according to JustEFAB. In our NLST cohort, non-graduates tended to be older than graduates, which is surprising since they tended to start smoking at an earlier age. This may be explained by biases in the age criteria for NLST eligibility. Studies have shown these criteria to potentially have excluded younger at-risk smokers with a high school diploma or less at a higher rate than more educated younger smokers, potentially reducing both the amount of non-graduates in our cohort and affecting their correlation with age (Castro et al., 2021).

4.5 Limitations

This study is primarily limited by the narrow availability of LDCT LCS datasets that are large, demographically diverse, and contain demographic data. In the NLST, the ratio of malignant LDCT scans to benign cases is relatively low, being around 10% in our validation datasets. While this is to be expected in a screening setting, the small number of scans with lung cancer limits our study's ability to examine smaller subgroups. This also limits our ability to examine the impact of multiple confounders on some demographic disparities (i.e. race), since splitting the NLST cohort by multiple risk factors can result in too few malignant scans within a subset for reliable analysis.

A low rate of lung cancer, combined with the fact that non-White participants only account for 7% of the NLST dataset, prevents us from examining the models' impact on Asian Americans, Native Americans, Native Hawaiians, and Hispanic or Latino participants. This underrepresentation is tied to biases in the pack-year thresholds in screening criteria against racial minorities (Aredo et al., 2022) and those with a lower SES (Castro et al., 2021), and makes it challenging to validate whether current models are potentially unfair across diverse populations. Alternative screening criteria, such as using a risk model for determining eligibility, has shown promise in reducing this racial bias (Choi et al., 2023), but there is a lack of large, diverse LDCT datasets reflecting such a change. This limits the data available to examine the Venkadesh21 model's racial disparities.

Additionally, we note that characteristics such as race, current smoking status, work history and previous diagnosis were self-reported by NLST participants and limited to the questionnaire provided by the NLST research team between 2002 and 2007. It is also important to remember that categories for race are imprecisely defined and based on the social context of where the data is collected (Mccradden et al., 2023). While the NLST collects an extensive list of characteristics from its participant questionnaire, other screening trials may be limited by their size (Wille et al., 2016), and relative lack of demographic information in the interest of privacy (van Bekkum, 2025).

4.6 Future Work

This study presents opportunities for multiple methods to mitigate biases in future work. For the Venkadesh21 model's racial bias, the JustEFAB framework recommends the most *upstream* solution, which in this case would be collecting new screening trial data with less biased criteria and ideally a larger percentage of non-White participants (Mccradden et al., 2023). More malignant scans from underrepresented groups can allow an intersectional analysis within racial groups, which is important since discrimination is often compounded on factors like race, sex, and socioeconomic status (Seyyed-Kalantari et al., 2021). However, in the absence of new screening data, a practical mitigation strategy may be to oversample the nodules from Black American participants during training using data augmentation to reduce the data imbalance (Bria et al., 2020).

If sex is considered to be an independent LC risk factor (Gasperino, 2011), future studies could add sex as part of Sybil's loss function, as a means to optimize performance for both men and women in training, or evaluate the utility of separate models for men and women in LCS. To reduce shortcut learning, some studies have proposed adversarial debiasing to train models to not predict certain characteristics (Yang et al., 2023), though this may remove clinically

relevant information useful for risk estimation (Brown et al., 2023). There is also potential for an ensemble of models (i.e. a nodule-based model and a full-lung model), which could show promise in reducing biases and increasing overall performance (Zhang et al., 2022). However, it should be noted that methods to mitigate bias can flatten relevant differences across the population and may result in lower overall performance, or increase the performance for one subgroup and reduce performance for others (Narayanan, 2018; Giovanola and Tiribelli, 2023).

Further investigation into the explainability of AI models is also key for fairness, since it can help practitioners and participants understand why a model gives a participant a specific prediction (Giovanola and Tiribelli, 2023; Mccradden et al., 2023; Richardson and Gilbert, 2021). This is particularly difficult in DL models, which are black-boxes due to their large numbers of parameters. Further research in developing and evaluating model explanations (Nauta et al., 2023) could uncover insights into their behavior, which may better inform radiologists into how much to trust the model's prediction for a particular scan.

4.7 State of Algorithmic Fairness in Screening Practice

We as AI researchers and developers chose one particular ethical framework for this study, and evaluated disparity between subgroups on metrics used in previous LCS AI studies (Venkadesh et al., 2021; Mikhael et al., 2023; Simon et al., 2023; McWilliams et al., 2013; Aredo et al., 2022). However, there must be careful considerations made in practice about what exactly is a fair AI tool for a screening setting. Studies interviewing AI developers have found that they are often ill-equipped to make these decisions alone (Richardson and Gilbert, 2021; Griffin et al., 2024). This is due in part to the large number of ethical definitions and frameworks for AI fairness (Mccradden et al., 2023; Obermeyer et al., 2021; Giovanola and Tiribelli, 2023; Barocas et al., 2023). These contain criteria which are often contradictory (Ferrara, 2024; Narayanan, 2018) or too abstract and detached from technical practice (Richardson and Gilbert, 2021). This can make fair AI development overwhelming and confusing for developers to navigate through, and often raises more questions than answers (Griffin et al., 2024).

This highlights the need for further research towards developing frameworks for fair AI decision-making in screening. Such frameworks should be backed by a shared and just definition of fairness, aligned with the expertise and values of screening stakeholders. These should also effectively translate ethical framing around AI fairness into actionable field-specific guidelines, since AI fairness and bias highly depends on the domain (Richardson and Gilbert, 2021). In medical screening, clinicians may argue for the usage of demographic characteristics like sex or race, since they may act

as a proxy for risk factors for lung cancer (i.e. environmental exposure, work history, hormone patterns) (Donington and Colson, 2011; Nakamura et al., 2011; Kreuzer et al., 2000). Additionally, proper mechanisms should be in place in organizations for flagging AI biases that would be harmful to participants (Mccradden et al., 2023; Obermeyer et al., 2021; Richardson and Gilbert, 2021). Such mechanisms should encourage developers and researchers to proactively develop fair AI systems, allow them to easily report unfair biases when detected, and provide guidelines for proper bias mitigation. Therefore, further development of fair AI systems for LCS requires interdisciplinary research and discussions between various stakeholders to determine norms around algorithmic fairness, which are then translated into priorities and practices at the organization level.

5. Conclusion

We uncovered four performance disparities in lung cancer risk estimation models investigated in this work which, according to the JustEFAB ethical framework, would lead to unfair outcomes for specific participant groups. The Sybil lung-based risk estimation model performed worse for men than women, even when controlling for the prevalence of known clinical confounders, despite men making up the majority of NLST participants. The Venkadesh21 nodule risk estimation model had a lower sensitivity for Black American participants, likely due to underrepresentation in NLST. Additionally, all models found had higher false positive rates for lower-BMI participants and those without a high school diploma or GED, who are already more likely to have lung cancer than those with a higher BMI or education status. These findings raise further questions about the relationships between these demographic characteristics and lung cancer risk factors and the downstream impact of biases in lung cancer screening criteria, and invite further research into the effectiveness of bias mitigation strategies. They also highlight the need for further discussions and interdisciplinary research on how to best apply processes to improve AI fairness in LCS, to ensure high quality diagnostic screening for all who may be at risk for lung cancer.

Acknowledgments

This study is part of the project ROBUST: Trustworthy AI-based Systems for Sustainable Growth (project number KICH3.L TP.20.006). The researchers received funding from: the Dutch Science Foundation, the Dutch Ministry of Economic Affairs, MeVis Medical Solutions (Bremen, Germany), Siemens Healthineers, the Fulbright U.S. Student Program and ELLIS. We also acknowledge important conversations with P.G.M. and E.Th.S. in this study.

Ethical Standards

The work follows appropriate ethical standards in conducting research and writing the manuscript, following all applicable laws and regulations regarding treatment of animals or human subjects.

Conflicts of Interest

S.G.: no relevant conflicts of interest. **M.V.:** funded by a public private project with funding from the Dutch Science Foundation, the Dutch Ministry of Economic Affairs, and MeVis Medical Solutions (Bremen, Germany). **A.H.:** no relevant conflicts of interest. **J.K.:** no relevant conflicts of interest. **C.J.:** research grants and royalties to host institution from MeVis Medical Solutions (Bremen, Germany); payment for lectures from Canon Medical Systems and Johnson & Johnson; collaborator in a public-private research project where Radboud University Medical Center collaborates with Philips Medical Systems (Best, the Netherlands). **L.P.:** reviewer for the FAIMI MELBA Special Fairness Issue. **F.v.d.G.:** funded by a public private project with funding from the Dutch Science Foundation, the Dutch Ministry of Economic Affairs, and MeVis Medical Solutions (Bremen, Germany).

Data availability

The National Lung Screening Trial (NLST) dataset is only accessible via request, as the data is not publicly available. Permission for this study was obtained from the NLST (National Lung Screening Trial Research Team et al., 2011) through the National Cancer Institute Cancer Data Access System (approved Project ID: NLST-1268 - Automated classification/ detection of Incidental Findings in LCS scans).

References

Sarah K. Abe, Saki Narita, Eiko Saito, Norie Sawada, Taichi Shimazu, Atsushi Goto, Taiki Yamaji, Motoki Iwasaki, Manami Inoue, and Shoichiro Tsugane. Body mass index, height, weight change, and subsequent lung cancer risk: The japan public health center-based prospective study. *Cancer Epidemiology, Biomarkers & Prevention*, 30(9):1708–1716, June 2021. ISSN 1538-7755. . URL <http://dx.doi.org/10.1158/1055-9965.EPI-21-0195>.

Jacqueline V Areo, Eunji Choi, Victoria Y Ding, Martin C Tammemägi, Kevin ten Haaf, Sophia J Luo, Neal D Freedman, Lynne R Wilkens, Loïc Le Marchand, Heather A Wakelee, Rafael Meza, Sung-Shim Lani Park, Iona Cheng, and Summer S Han. Racial and ethnic disparities in lung

cancer screening by the 2021 uspstf guidelines versus risk-based criteria: The multiethnic cohort study. *JNCI Cancer Spectrum*, 6(3), May 2022. ISSN 2515-5091. . URL <http://dx.doi.org/10.1093/jncics/pkac033>.

David R. Baldwin. Management of pulmonary nodules according to the 2015 british thoracic society guidelines. key messages for clinical practice. *Polish Archives of Internal Medicine*, 126(4):262–274, April 2016. ISSN 1897-9483. . URL <http://dx.doi.org/10.20452/pamw.3379>.

Solon Barocas, Moritz Hardt, and Arvind Narayanan. *Fairness and Machine Learning: Limitations and Opportunities*. MIT Press, 2023.

Mélanie Bernhardt, Charles Jones, and Ben Glocker. Potential sources of dataset bias complicate investigation of underdiagnosis by machine learning algorithms. *Nature Medicine*, 28(6):1157–1158, June 2022. ISSN 1546-170X. . URL <http://dx.doi.org/10.1038/s41591-022-01846-8>.

Alessandro Bria, Claudio Marrocco, and Francesco Torella. Addressing class imbalance in deep learning for small lesion detection on medical images. *Computers in Biology and Medicine*, 120:103735, May 2020. ISSN 0010-4825. . URL <http://dx.doi.org/10.1016/j.combiomed.2020.103735>.

Alexander Brown, Nenad Tomasev, Jan Freyberg, Yuan Liu, Alan Karthikesalingam, and Jessica Schrouff. Detecting shortcut learning for fair medical ai using shortcut testing. *Nature Communications*, 14(1), July 2023. ISSN 2041-1723. . URL <http://dx.doi.org/10.1038/s41467-023-39902-7>.

R. J. M. Bruls and R. M. Kwee. Workload for radiologists during on-call hours: dramatic increase in the past 15 years. *Insights into Imaging*, 11(1), November 2020. ISSN 1869-4101. . URL <http://dx.doi.org/10.1186/s13244-020-00925-z>.

Samuel Castro, Ernesto Sosa, Vanessa Lozano, Aamna Akhtar, Kyra Love, Jeanette Duffels, Dan J. Raz, Jae Y. Kim, Virginia Sun, and Loretta Erhunmwunsee. The impact of income and education on lung cancer screening utilization, eligibility, and outcomes: a narrative review of socioeconomic disparities in lung cancer screening. *Journal of Thoracic Disease*, 13(6):3745–3757, June 2021. ISSN 2077-6624. . URL <http://dx.doi.org/10.21037/jtd-20-3281>.

S. Chen, W.L. Lin, W.T. Liu, L.Y. Zou, Y. Chen, and F. Lu. Pulmonary nodule malignancy probability: a meta-analysis of the brock model. *Clinical Radiology*, 82: 106788, March 2025. ISSN 0009-9260. . URL <http://dx.doi.org/10.1016/j.crad.2024.106788>.

Eunji Choi, Victoria Y. Ding, Sophia J. Luo, Kevin ten Haaf, Julie T. Wu, Jacqueline V. Areo, Lynne R. Wilkens, Neal D. Freedman, Leah M. Backhus, Ann N. Leung, Rafael Meza, Natalie S. Lui, Christopher A. Haiman, Sung-Shim Lani Park, Loïc Le Marchand, Joel W. Neal, Iona Cheng, Heather A. Wakelee, Martin C. Tammemägi, and Summer S. Han. Risk model-based lung cancer screening and racial and ethnic disparities in the us. *JAMA Oncology*, 9(12):1640, December 2023. ISSN 2374-2437. . URL <http://dx.doi.org/10.1001/jamaoncol.2023.4447>.

Alexandra Chouldechova and Aaron Roth. A snapshot of the frontiers of fairness in machine learning. *Communications of the ACM*, 63(5):82–89, April 2020. ISSN 1557-7317. . URL <http://dx.doi.org/10.1145/3376898>.

Patricia M. de Groot, Carol C. Wu, Brett W. Carter, and Reginald F. Munden. The epidemiology of lung cancer. *Translational Lung Cancer Research*, 7(3):220–233, June 2018. ISSN 2226-4477. . URL <http://dx.doi.org/10.21037/tlcr.2018.05.06>.

Harry J. de Koning, Carlijn M. van der Aalst, Pim A. de Jong, Ernst T. Scholten, Kristiaan Nackaerts, Marjolein A. Heuvelmans, Jan-Willem J. Lammers, Carla Weenink, Uraujh Yousaf-Khan, Nanda Horeweg, Susan van 't Westeinde, Mathias Prokop, Willem P. Mali, Firdaus A.A. Mohamed Hoessein, Peter M.A. van Ooijen, Joachim G.J.V. Aerts, Michael A. den Bakker, Erik Thunnissen, Johny Verschakelen, Rozemarijn Vliegenthart, Joan E. Walter, Kevin ten Haaf, Harry J.M. Groen, and Matthijs Oudkerk. Reduced lung-cancer mortality with volume ct screening in a randomized trial. *New England Journal of Medicine*, 382(6):503–513, February 2020. ISSN 1533-4406. . URL <http://dx.doi.org/10.1056/NEJMoa1911793>.

Jessica S. Donington and Yolonda L. Colson. Sex and gender differences in non-small cell lung cancer. *Seminars in Thoracic and Cardiovascular Surgery*, 23(2):137–145, June 2011. ISSN 1043-0679. . URL <http://dx.doi.org/10.1053/j.semcts.2011.07.001>.

Mariam El-Zein, Marie-Elise Parent, Belinda Nicolau, Anita Koushik, Jack Siemiatycki, and Marie-Claude Rousseau. Body mass index, lifetime smoking intensity and lung cancer risk. *International Journal of Cancer*, 133(7): 1721–1731, April 2013. ISSN 1097-0215. . URL <http://dx.doi.org/10.1002/ijc.28185>.

Loretta Erhunmwunsee, Mary-Beth M. Joshi, Debbi H. Conlon, and David H. Harpole. Neighborhood-level socioeconomic determinants impact outcomes in nonsmall

cell lung cancer patients in the southeastern united states. *Cancer*, 118(20):5117–5123, March 2012. ISSN 1097-0142. . URL <http://dx.doi.org/10.1002/cncr.26185>.

Emilio Ferrara. Fairness and bias in artificial intelligence: A brief survey of sources, impacts, and mitigation strategies. *Sci*, 6(1), 2024. ISSN 2413-4155. . URL <https://www.mdpi.com/2413-4155/6/1/3>.

James Gasperino. Gender is a risk factor for lung cancer. *Medical Hypotheses*, 76(3):328–331, March 2011. ISSN 0306-9877. . URL <http://dx.doi.org/10.1016/j.mehy.2010.10.030>.

Benedetta Giovanola and Simona Tiribelli. Beyond bias and discrimination: redefining the AI ethics principle of fairness in healthcare machine-learning algorithms. *AI & SOCIETY*, 38(2):549–563, April 2023. ISSN 1435-5655. . URL <https://doi.org/10.1007/s00146-022-01455-6>.

Tricia A Griffin, Brian P Green, and Jos V M Welie. The ethical wisdom of AI developers. *AI Ethics*, March 2024.

S. Gu, R. Li, J.K. Leader, B. Zheng, J. Bon, D. Gur, F. Sciurba, C. Jin, and J. Pu. Obesity and extent of emphysema depicted at ct. *Clinical Radiology*, 70(5):e14–e19, May 2015. ISSN 0009-9260. . URL <http://dx.doi.org/10.1016/j.crad.2015.01.007>.

J A Hanley and B J McNeil. The meaning and use of the area under a receiver operating characteristic (roc) curve. *Radiology*, 143(1):29–36, April 1982. ISSN 1527-1315. . URL <http://dx.doi.org/10.1148/radiology.143.1.7063747>.

Jay A. Harolds, Jay R. Parikh, Edward I. Bluth, Sharon C. Dutton, and Michael P. Recht. Burnout of radiologists: Frequency, risk factors, and remedies: A report of the acr commission on human resources. *Journal of the American College of Radiology*, 13(4):411–416, April 2016. ISSN 1546-1440. . URL <http://dx.doi.org/10.1016/j.jacr.2015.11.003>.

Ward Hendrix, Nils Hendrix, Ernst T. Scholten, Mariëlle Mourits, Joline Trap-de Jong, Steven Schalekamp, Mike Korst, Maarten van Leuken, Bram van Ginneken, Mathias Prokop, Matthieu Rutten, and Colin Jacobs. Deep learning for the detection of benign and malignant pulmonary nodules in non-screening chest ct scans. *Communications Medicine*, 3(1), October 2023. ISSN 2730-664X. . URL <http://dx.doi.org/10.1038/s43856-023-00388-5>.

Hussein Ibrahim, Xiaoxuan Liu, Nevine Zariffa, Andrew D Morris, and Alastair K Denniston. Health data poverty: an assailable barrier to equitable digital health care. *The Lancet Digital Health*, 3(4):e260–e265, April 2021. ISSN 2589-7500. . URL [http://dx.doi.org/10.1016/S2589-7500\(20\)30317-4](http://dx.doi.org/10.1016/S2589-7500(20)30317-4).

Charles Jones, Daniel C. Castro, Fabio De Sousa Ribeiro, Ozan Oktay, Melissa McCradden, and Ben Glocker. A causal perspective on dataset bias in machine learning for medical imaging. *Nature Machine Intelligence*, 6(2):138–146, Feb 2024. ISSN 2522-5839. . URL <https://doi.org/10.1038/s42256-024-00797-8>.

Kleanthis Konstantinidis. The shortage of radiographers: A global crisis in healthcare. *Journal of Medical Imaging and Radiation Sciences*, 55(4):101333, December 2024. ISSN 1939-8654. . URL <http://dx.doi.org/10.1016/j.jmir.2023.10.001>.

M Kreuzer, P Boffetta, E Whitley, W Ahrens, V Gaborieau, J Heinrich, K H Jöckel, L Kreienbrock, S Mallone, F Merletti, F Roesch, P Zambon, and L Simonato. Gender differences in lung cancer risk by smoking: a multicentre case-control study in germany and italy. *British Journal of Cancer*, 82(1):227–233, January 2000. ISSN 1532-1827. . URL <http://dx.doi.org/10.1054/bjoc.1999.0904>.

Harriet L. Lancaster, Beibei Jiang, Michael P.A. Davies, Jan Willem C. Gratama, Mario Silva, Jaeyoun Yi, Marjolein A. Heuvelmans, Geertruida H. de Bock, Anand Devaraj, John K. Field, and Matthijs Oudkerk. Histological proven ai performance in the ukls ct lung cancer screening study: Potential for workload reduction. *European Journal of Cancer*, 220:115324, 2025. ISSN 0959-8049. . URL <https://www.sciencedirect.com/science/article/pii/S0959804925001054>.

Huyen Le, Colinda C.J.M. Simons, and Piet A. van den Brandt. The association between height and risk of lung cancer subtypes in men and women in the netherlands cohort study. *Cancer Epidemiology*, 92:102613, October 2024. ISSN 1877-7821. . URL <http://dx.doi.org/10.1016/j.canep.2024.102613>.

Kuan Pin Lim, Henry Marshall, Martin Tammemägi, Fraser Brims, Annette McWilliams, Emily Stone, Renee Manser, Karen Canfell, Marianne Weber, Luke Connelly, Rayleen V. Bowman, Ian A. Yang, Paul Fogarty, John Mayo, John Yee, Renelle Myers, Sukhinder Atkar-Khattra, David C. L. Lam, Antoni Rosell, Christine D. Berg, Kwun M. Fong, Stephen Lam, Kwun M. Fong, Ian Yang, Rayleen Bowman, Richard Slaughter, Katrina Hopcroft, Linda Passmore, Elizabeth McCaul, Susanna

Doyle, Henry Marshall, Rachael O'Rourke, Luke Connelly, Karin Steinke, Renee Manser, Paul Fogarty, Daniel Steinfort, Louis Irving, Katharine See, Diane Pascoe, Mark McCusker, Paul Mitchell, Annette McWilliams, Fraser Brims, Kuan Pin Lim, Emily Stone, Matthew Peters, Klaire Garnica, Lisa Tarlinton, Robert Kent, Karen Canfell, Marianne Weber, Nicole Rankin, Yoon-Jung Kang, Martin Tammemägi, Stephen Lam, John Yee, Renelle Myers, John Mayo, Ren Yuan, John English, Sonya Cressman, Sukhinder Atkar-Khattra, David C. L. Lam, Antoni Rossell, and Christine Berg. Protocol and rationale for the international lung screening trial. *Annals of the American Thoracic Society*, 17(4):503–512, April 2020. ISSN 2325-6621. . URL <http://dx.doi.org/10.1513/AnnalsATS.201902-1020C>.

Lauren May, Kathryn Shows, Patrick Nana-Sinkam, Howard Li, and Joseph W. Landry. Sex differences in lung cancer. *Cancers*, 15(12):3111, June 2023. ISSN 2072-6694. . URL <http://dx.doi.org/10.3390/cancers15123111>.

Melissa Mccradden, Oluwadara Odusi, Shalmali Joshi, Ismail Akrout, Kagiso Ndlovu, Ben Glocke, Gabriel Maicas, Xiaoxuan Liu, Mjaye Mazwi, Tee Garnett, Lauren Oakden-Rayner, Myrtede Alfred, Irvine Sihlahla, Oswa Shafei, and Anna Goldenberg. What's fair is... fair? presenting justefab, an ethical framework for operationalizing medical ethics and social justice in the integration of clinical machine learning: Justefab. In *Proceedings of the 2023 ACM Conference on Fairness, Accountability, and Transparency*, FAccT '23, page 1505–1519, New York, NY, USA, 2023. Association for Computing Machinery. ISBN 9798400701924. . URL <https://doi.org/10.1145/3593013.3594096>.

Annette McWilliams, Martin C. Tammemagi, John R. Mayo, Heidi Roberts, Geoffrey Liu, Kam Soghrati, Kazuhiro Yasufuku, Simon Martel, Francis Laberge, Michel Gingras, Sukhinder Atkar-Khattra, Christine D. Berg, Ken Evans, Richard Finley, John Yee, John English, Paola Nasute, John Goffin, Serge Puksa, Lori Stewart, Scott Tsai, Michael R. Johnston, Daria Manos, Garth Nicholas, Glenwood D. Goss, Jean M. Seely, Kayvan Amjadi, Alain Tremblay, Paul Burrowes, Paul MacEachern, Rick Bhatia, Ming-Sound Tsao, and Stephen Lam. Probability of Cancer in Pulmonary Nodules Detected on First Screening CT. *New England Journal of Medicine*, 369(10):910–919, September 2013. ISSN 0028-4793. . URL <https://doi.org/10.1056/NEJMoa1214726>. Publisher: Massachusetts Medical Society _eprint: <https://doi.org/10.1056/NEJMoa1214726>.

Peter G. Mikhael, Jeremy Wohlwend, Adam Yala, Ludvig Karstens, Justin Xiang, Angelo K. Takigami, Patrick P. Bourgouin, PuiYee Chan, Sofiane Mrah, Wael Amayri, Yu-Hsiang Juan, Cheng-Ta Yang, Yung-Liang Wan, Gigin Lin, Lecia V. Sequist, Florian J. Fintelmann, and Regina Barzilay. Sybil: A Validated Deep Learning Model to Predict Future Lung Cancer Risk From a Single Low-Dose Chest Computed Tomography. *Journal of Clinical Oncology*, 41(12):2191–2200, April 2023. ISSN 0732-183X. . URL <https://www.ncbi.nlm.nih.gov/pmc/articles/PMC10419602/>.

Virginia A. Moyer. Screening for lung cancer: U.s. preventive services task force recommendation statement. *Annals of Internal Medicine*, 160(5):330–338, March 2014. ISSN 1539-3704. . URL <http://dx.doi.org/10.7326/m13-2771>.

Haruhiko Nakamura, Koji Ando, Takuo Shinmyo, Katsumi Morita, Atsushi Mochizuki, Noriaki Kurimoto, and Shinobu Tatsunami. Female gender is an independent prognostic factor in non-small-cell lung cancer: A meta-analysis. *Annals of Thoracic and Cardiovascular Surgery*, 17(5):469–480, 2011. ISSN 2186-1005. . URL <http://dx.doi.org/10.5761/atcs.oa.10.01637>.

Arvind Narayanan. Translation tutorial: 21 fairness definitions and their politics. In *Proceedings of the Conference on Fairness, Accountability and Transparency*, volume 1170, page 3, New York, USA, 2018.

National Lung Screening Trial Research Team, Denise R. Aberle, Amanda M. Adams, Christine D. Berg, William C. Black, Jonathan D. Clapp, Richard M. Fagerstrom, Ilana F. Gareen, Constantine Gatsonis, Pamela M. Marcus, and JoRean D. Sicks. Reduced lung-cancer mortality with low-dose computed tomographic screening. *The New England Journal of Medicine*, 365(5):395–409, August 2011. ISSN 1533-4406. .

Meike Nauta, Jan Trienes, Shreyasi Pathak, Elisa Nguyen, Michelle Peters, Yasmin Schmitt, Jörg Schlötterer, Maurice van Keulen, and Christin Seifert. From anecdotal evidence to quantitative evaluation methods: A systematic review on evaluating explainable ai. *ACM Computing Surveys*, 55(13s):1–42, July 2023. ISSN 1557-7341. . URL <https://doi.org/10.1145/3583558>.

Ainsley J. Newson. *Population screening*, page 118–142. Cambridge University Press, June 2011. ISBN 9780511862670. . URL <http://dx.doi.org/10.1017/CBO9780511862670>.

Ziad Obermeyer, Brian Powers, Christine Vogeli, and Sendhil Mullainathan. Dissecting racial bias in an algorithm used to manage the health of populations. *Science*, 366 (6464):447–453, 2019. . URL <https://www.science.org/doi/abs/10.1126/science.aax2342>.

Ziad Obermeyer, Rebecca Nissan, Michael Stern, Stephanie Eanoff, Emily Joy Bembeneck, and Sendhil Mullainathan. Algorithmic bias playbook. *Center for Applied AI at Chicago Booth*, pages 7–8, 2021.

World Health Organization. Surveillance of chronic disease risk factors : country level data and comparable estimates, 2005.

Paul F. Pinsky, Timothy R. Church, Grant Izmirlian, and Barnett S. Kramer. The national lung screening trial: Results stratified by demographics, smoking history, and lung cancer histology. *Cancer*, 119(22):3976–3983, August 2013. ISSN 1097-0142. . URL <http://dx.doi.org/10.1002/cncr.28326>.

Brianna Richardson and Juan E Gilbert. A framework for fairness: A systematic review of existing fair ai solutions. *arXiv preprint arXiv:2112.05700*, 2021.

Laleh Seyyed-Kalantari, Haoran Zhang, Matthew B. A. McDermott, Irene Y. Chen, and Marzyeh Ghassemi. Under-diagnosis bias of artificial intelligence algorithms applied to chest radiographs in under-served patient populations. *Nature Medicine*, 27(12):2176–2182, December 2021. ISSN 1546-170X. . URL <https://doi.org/10.1038/s41591-021-01595-0>.

E. Shum, N. Florez, J. Brahmer, C. Aggarwal, H. Wakelee, M. Chau, R. Shenolikar, R. Salomonsen, J. Chaieb, L. Luciani-Silverman, D. Guy, L. Woldmann, A.-A. Cirtel, and S. Peters. P4.04d.01 gender disparities in lung cancer screening: A systematic literature review. *Journal of Thoracic Oncology*, 19(10):S371, October 2024. ISSN 1556-0864. . URL <http://dx.doi.org/10.1016/j.jtho.2024.09.669>.

Jill M Siegfried. Sex and gender differences in lung cancer and chronic obstructive lung disease. *Endocrinology*, 163(2):bqab254, 12 2021. ISSN 0013-7227. .

Judit Simon, Peter Mikhael, Ismail Tahir, Alexander Gaur, Stefan Ringer, Amanda Fata, Yang Chi-Fu Jeffrey, Jo-Anne Shepard, Francine Jacobson, Regina Barzilay, Leicia V. Sequist, Lydia E. Pace, and Florian J. Fintelmann. Role of sex in lung cancer risk prediction based on single low-dose chest computed tomography. *Scientific Reports*, 13(1), October 2023. ISSN 2045-2322. . URL <http://dx.doi.org/10.1038/s41598-023-45671-6>.

Llewellyn Smith, Louise A. Brinton, Margaret R. Spitz, Tram Kim Lam, Yikyung Park, Albert R. Hollenbeck, Neal D. Freedman, and Gretchen L. Gierach. Body mass index and risk of lung cancer among never, former, and current smokers. *JNCI: Journal of the National Cancer Institute*, 104(10):778–789, March 2012. ISSN 0027-8874. . URL <http://dx.doi.org/10.1093/jnci/djs179>.

Christine S. Spencer, Darrell J. Gaskin, and Eric T. Roberts. The quality of care delivered to patients within the same hospital varies by insurance type. *Health Affairs*, 32(10):1731–1739, October 2013. ISSN 1544-5208. . URL <http://dx.doi.org/10.1377/hlthaff.2012.1400>.

Marvin van Bekkum. Using sensitive data to de-bias ai systems: Article 10(5) of the eu ai act. *Computer Law & Security Review*, 56:106115, April 2025. ISSN 2212-473X. . URL <http://dx.doi.org/10.1016/j.clsr.2025.106115>.

Kiran Vaidhya Venkadesh, Arnaud A. A. Setio, Anton Schreuder, Ernst T. Scholten, Kaman Chung, Mathilde M. W. Wille, Zaigham Saghir, Bram van Ginneken, Mathias Prokop, and Colin Jacobs. Deep Learning for Malignancy Risk Estimation of Pulmonary Nodules Detected at Low-Dose Screening CT. *Radiology*, 300(2):438–447, August 2021. ISSN 0033-8419. . URL <https://pubs.rsna.org/doi/full/10.1148/radiol.2021204433>. Publisher: Radiological Society of North America.

Mathilde M. W. Wille, Asger Dirksen, Haseem Ashraf, Zaigham Saghir, Karen S. Bach, John Brodersen, Paul F. Clementsen, Hanne Hansen, Klaus R. Larsen, Jann Mortensen, Jakob F. Rasmussen, Niels Seersholm, Birgit G. Skov, Laura H. Thomsen, Philip Tønnesen, and Jesper H. Pedersen. Results of the Randomized Danish Lung Cancer Screening Trial with Focus on High-Risk Profiling. *American Journal of Respiratory and Critical Care Medicine*, 193(5):542–551, March 2016. ISSN 1535-4970. .

Jenny Yang, Andrew A. S. Soltan, David W. Eyre, Yang Yang, and David A. Clifton. An adversarial training framework for mitigating algorithmic biases in clinical machine learning. *npj Digital Medicine*, 6(1), March 2023. ISSN 2398-6352. . URL <http://dx.doi.org/10.1038/s41746-023-00805-y>.

Kuan Zhang, Bardia Khosravi, Sanaz Vahdati, Shahriar Faghani, Fred Nugen, Seyed Moein Rassoulinejad-Mousavi, Mana Moassefi, Jaidip Manikrao M. Jagtap, Yashbir Singh, Pouria Rouzrokh, and Bradley J. Erickson. Mitigating bias in radiology machine learning: 2. model development. *Radiology: Artificial Intelligence*, 4(5), September 2022. ISSN 2638-6100. . URL <http://dx.doi.org/10.1148/ryai.220010>.

Appendix A. NLST Training Datasets for Venkadesh21 and Sybil

While both Venkadesh21 (Venkadesh et al., 2021) and Sybil (Mikhael et al., 2023) were trained on NLST data, they were trained on different subsets suited to the design choices made for each model. Since Venkadesh21 is a nodule risk estimation model, its authors chose a set of NLST scans with visible nodules which could be retrospectively located and annotated. The lung cancer labels for this dataset, along with our experiment's validation set, were determined by whether the patient received a lung cancer diagnosis. Venkadesh21's full NLST training dataset contains 16,077 nodules across 10,183 scans, which was used in 10-fold cross validation to create an ensemble of models. Demographic characteristics for this full set are shown in Table 7.

Sybil was trained on a scan-level NLST subset, where only some scans contained visible nodules. Its labels were determined for each scan separately, with malignancy at each year based on the days between when a scan was collected and when a participant was diagnosed with lung cancer. Sybil's NLST dataset is split into training ($n=28,162$ scans), development ($n=6,839$), and test sets ($n=6,282$). Demographics for Sybil's training set are shown in Table 8.

Based on information provided for us in this study, we successfully recovered information about all samples from the Venkadesh21 NLST dataset, and all but three samples from the Sybil NLST dataset. We found that from the Venkadesh21 set, 4,271 LDCT scans are in Sybil's training set, 947 in its development set, and 757 in its testing set. This leaves 35,305 other scans in Sybil's datasets, and 4,208 scans from Venkadesh21's dataset not found in any of Sybil's sets. For our experiments, we used NLST validation predictions from Venkadesh21 (each prediction from only a single fold), so the dataset used for this study included the 5,912 LDCT scans in the Venkadesh21 cross-validation set which were not included in Sybil's training set. We successfully gathered predictions from all but one of these scans, resulting in 5,911 validation predictions.

Examining both Tables 7 and 8 shows that the demographic characteristics are almost identical between the two models' training sets, and with the validation set used for our study, with almost all subgroups having smaller than a 2% difference between datasets. This indicates very little population shift, and that the validation set is representative of both models' training sets. The only exception to this is that in the Sybil training set, its malignant scans contain about 4% more scans from high school graduates and GED recipients (28.8%) than the Venkadesh21 set (25.0%), and about 2% fewer malignant scans each from Bachelor's degree holders and participants who went to graduate school.

Appendix B. Fairness Assessment Results

Here, we report comprehensive results for assessing whether demographic performance disparities found in the subgroup performance analysis were confounded by the 10 factors with the highest prevalence disparities between subgroups.

For Sybil's disparity between men and women, Table 9 displays the 10 factors with the greatest prevalence disparity and their impact on Sybil's AUROC for men and women. Table 10 displays the impact of these factors on sensitivity (at 90% specificity) and specificity (at 90% sensitivity).

For Venkadesh21's performance disparity between White and Black participants, Table 11 displays the 10 factors with the greatest prevalence disparity and their impact on Venkadesh21's AUROC for racial groups. Table 12 displays the impact of these potential confounders on sensitivity (at 90% specificity) and specificity (at 90% sensitivity).

For the disparity between participants with high BMI and those with low BMI, Table 13 displays the 10 factors with the greatest prevalence disparity and their impact on Sybil's AUROC for these groups. Table 14 displays the impact of these potential confounders on sensitivity (at a 90% specificity threshold) and specificity (at a 90% sensitivity threshold) for Sybil. Table 15 displays the impact of these same factors on PanCan2b's significant disparity between high-BMI and low-BMI participants. Additionally, Figure 7 displays Sybil's ROC curves reporting a significant performance disparity when emphysema is in a LDCT.

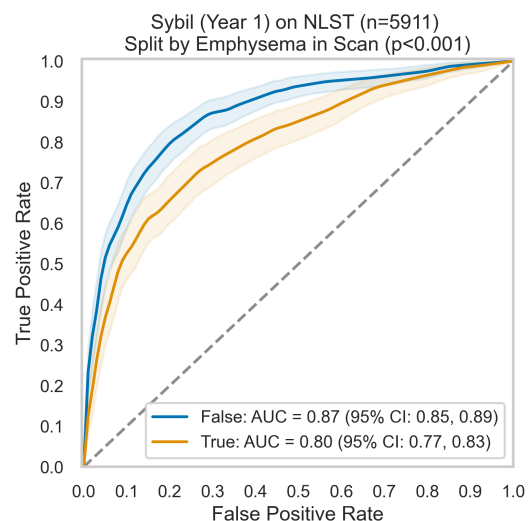


Figure 7: ROC curves (with 95% CIs) for Sybil (Year 1), split by emphysema, in NLST ($n=5911$ scans).

Table 16 displays the 10 factors with the highest prevalence disparities based on education status (and AUROC for PanCan2b), while sensitivity and specificity (when isolating and excluding these factors) is displayed for each model in Tables 17 (Venkadesh21), 18 (Sybil) and 19 (PanCan2b).

Table 7: Demographics of the NLST training set used for Venkadesh21 (n=10183 scans). HS = High School.

Characteristic	Subgroup	Malignant (n=1199)	Benign (n=8984)	All Scans (n=10183)
Education Status	8th grade or less	24 (2.0)	140 (1.6)	164 (1.6)
	9th-11th grade	68 (5.7)	450 (5.0)	518 (5.1)
	Associate Degree	295 (24.6)	1992 (22.2)	2287 (22.5)
	Bachelors Degree	182 (15.2)	1403 (15.6)	1585 (15.6)
	Graduate School	134 (11.2)	1331 (14.8)	1465 (14.4)
	HS Graduate / GED	300 (25.0)	2238 (24.9)	2538 (24.9)
Race	Post-HS training	171 (14.3)	1275 (14.2)	1446 (14.2)
	Asian	19 (1.6)	150 (1.7)	169 (1.7)
	Black	56 (4.7)	282 (3.1)	338 (3.3)
	More than one race	10 (0.8)	101 (1.1)	111 (1.1)
	Native American	9 (0.8)	34 (0.4)	43 (0.4)
	Native Hawaiian	2 (0.2)	31 (0.3)	33 (0.3)
Ethnicity	White	1101 (91.8)	8360 (93.1)	9461 (92.9)
	Hispanic/Latino	9 (0.8)	141 (1.6)	150 (1.5)
Sex	Not Hispanic/Latino	1180 (98.4)	8797 (97.9)	9977 (98.0)
	Female	501 (41.8)	3848 (42.8)	4349 (42.7)
Weight	Male	698 (58.2)	5136 (57.2)	5834 (57.3)
	Median (IQR)	174 (50)	180 (50)	180 (50)
Height	Median (IQR)	68 (6)	68 (6)	68 (6)
Body Mass Index	Median (IQR)	26 (4)	27 (6)	27 (6)
Age	Median (IQR)	64 (8)	62 (8)	62 (8)

Table 8: Demographics of the NLST training set used for Sybil (n=28160 scans). HS = High School.

Characteristic	Subgroup	Malignant (n=1444)	Benign (n=26716)	All Scans (n=28160)
Education Status	8th grade or less	42 (2.9)	311 (1.2)	353 (1.3)
	9th-11th grade	76 (5.3)	1189 (4.5)	1265 (4.5)
	Associate Degree	335 (23.2)	6312 (23.6)	6647 (23.6)
	Bachelors Degree	191 (13.2)	4645 (17.4)	4836 (17.2)
	Graduate School	129 (8.9)	3847 (14.4)	3976 (14.1)
	HS Graduate / GED	416 (28.8)	6165 (23.1)	6581 (23.4)
Race	Post-HS training	224 (15.5)	3767 (14.1)	3991 (14.2)
	Asian	23 (1.6)	552 (2.1)	575 (2.0)
	Black	68 (4.7)	968 (3.6)	1036 (3.7)
	More than one race	13 (0.9)	352 (1.3)	365 (1.3)
	Native American	6 (0.4)	90 (0.3)	96 (0.3)
	Native Hawaiian	1 (0.1)	69 (0.3)	70 (0.2)
Ethnicity	White	1333 (92.3)	24586 (92.0)	25919 (92.0)
	Hispanic/Latino	10 (0.7)	505 (1.9)	515 (1.8)
Sex	Not Hispanic/Latino	1423 (98.5)	26106 (97.7)	27529 (97.8)
	Female	604 (41.8)	10984 (41.1)	11588 (41.2)
Weight	Male	840 (58.2)	15732 (58.9)	16572 (58.8)
	Median (IQR)	175 (50)	180 (53)	180 (53)
Height	Median (IQR)	68 (6)	68 (6)	68 (6)
Body Mass Index	Median (IQR)	26 (5)	27 (6)	27 (6)
Age	Median (IQR)	63 (9)	61 (8)	61 (8)

Table 9: The top 10 characteristics with the largest prevalence difference between sexes, and the AUROC scores of the Sybil (Year 1) model between men and women, isolating for them.

Confounder	Subset	Male				Female				p
		Mal	Ben	Total %	AUROC	Mal	Ben	Total %	AUROC	
Height	> 68	257	2364	76.2	0.80 (0.77, 0.83)	10	136	5.9	0.84 (0.69, 0.96)	.63
	≤ 68	80	740	23.8	0.84 (0.79, 0.88)	234	2090	94.1	0.88 (0.86, 0.90)	.17
Weight	> 180	211	2015	64.7	0.83 (0.80, 0.86)	36	554	23.9	0.86 (0.77, 0.93)	.44
	≤ 180	126	1089	35.3	0.77 (0.72, 0.82)	208	1672	76.1	0.88 (0.86, 0.90)	< .001
Smoked Pipe	False	197	1967	62.9	0.82 (0.79, 0.85)	239	2172	97.6	0.88 (0.85, 0.90)	.01
	True	138	1118	36.5	0.80 (0.76, 0.84)	5	40	1.8	0.97 (0.93, 1.00)	.002
Smoked Cigars	True	102	963	31.0	0.79 (0.74, 0.83)	7	76	3.4	0.97 (0.92, 1.00)	.001
	False	233	2127	68.6	0.82 (0.79, 0.86)	237	2141	96.3	0.88 (0.85, 0.90)	.01
Work w/o Mask	False	228	2029	65.6	0.82 (0.79, 0.85)	214	1936	87.0	0.89 (0.87, 0.91)	< .001
	True	109	1075	34.4	0.79 (0.74, 0.84)	30	290	13.0	0.79 (0.69, 0.87)	.92
Pack-Years	≤ 55	141	1601	50.6	0.81 (0.77, 0.85)	144	1504	66.7	0.87 (0.83, 0.90)	.06
	> 55	196	1503	49.4	0.80 (0.77, 0.84)	100	722	33.3	0.90 (0.86, 0.93)	< .001
BMI	< 25	92	811	26.2	0.76 (0.70, 0.82)	117	879	40.3	0.85 (0.81, 0.89)	.009
	≥ 25	245	2293	73.8	0.83 (0.80, 0.86)	127	1347	59.7	0.90 (0.87, 0.93)	.003
Cigarettes per Day	≤ 25	141	1473	46.9	0.80 (0.76, 0.84)	139	1366	60.9	0.86 (0.82, 0.89)	.06
	> 25	196	1631	53.1	0.82 (0.78, 0.85)	105	860	39.1	0.91 (0.88, 0.94)	< .001
Lived w/ Smoker	False	43	498	15.7	0.81 (0.74, 0.89)	21	103	5.0	0.85 (0.75, 0.93)	.63
	True	292	2585	83.6	0.81 (0.78, 0.84)	222	2112	94.5	0.88 (0.86, 0.91)	< .001
Pneumonia Diag.	True	55	597	18.9	0.68 (0.59, 0.77)	81	649	29.6	0.86 (0.81, 0.90)	< .001
	False	281	2502	80.9	0.84 (0.81, 0.86)	157	1574	70.1	0.90 (0.87, 0.92)	.007

Table 10: Sensitivity and Specificity at specific thresholds (with 95% confidence intervals) for the Sybil (Year 1) model between men and women, isolating for the top 10 characteristics with the largest prevalence difference between sexes. Single asterisk (*) = metric of one subgroup is outside the CI of the other. Double asterisks (**) = CIs do not intersect.

Confounder	Subset	Sensitivity (90% Overall Specificity)			Specificity (90% Overall Sensitivity)		
		Male	Female	CI	Male	Female	CI
Height	> 68	0.52 (0.46, 0.59)	0.60 (0.29, 0.92)	0.45 (0.43, 0.47)	0.47 (0.39, 0.56)		
	≤ 68	0.55 (0.45, 0.67)	0.66 (0.60, 0.72)	0.49 (0.46, 0.53)	0.57 (0.55, 0.59)	**	
Weight	> 180	0.56 (0.49, 0.62)	0.64 (0.47, 0.80)	0.48 (0.46, 0.51)	0.63 (0.59, 0.67)	**	
	≤ 180	0.48 (0.39, 0.56)	0.66 (0.59, 0.72)	**	0.42 (0.39, 0.45)	0.54 (0.52, 0.56)	**
Smoked Pipe	False	0.56 (0.49, 0.63)	0.65 (0.59, 0.71)	*	0.46 (0.44, 0.48)	0.56 (0.54, 0.58)	**
	True	0.49 (0.40, 0.57)	1.00 (1.00, 1.00)	**	0.47 (0.44, 0.50)	0.47 (0.33, 0.62)	
Smoked Cigars	False	0.56 (0.50, 0.62)	0.65 (0.59, 0.71)	*	0.46 (0.43, 0.48)	0.56 (0.53, 0.58)	**
	True	0.45 (0.36, 0.54)	0.86 (0.50, 1.00)	*	0.48 (0.45, 0.51)	0.67 (0.56, 0.77)	**
Work w/o Mask	False	0.53 (0.46, 0.60)	0.68 (0.62, 0.75)	**	0.48 (0.46, 0.50)	0.57 (0.55, 0.59)	**
	True	0.52 (0.43, 0.61)	0.47 (0.30, 0.65)		0.43 (0.40, 0.46)	0.52 (0.46, 0.57)	**
Pack-Years	> 55	0.54 (0.47, 0.60)	0.73 (0.64, 0.82)	**	0.43 (0.41, 0.46)	0.54 (0.50, 0.58)	**
	≤ 55	0.52 (0.44, 0.60)	0.60 (0.52, 0.69)	*	0.49 (0.47, 0.52)	0.57 (0.55, 0.60)	**
BMI	< 25	0.50 (0.40, 0.60)	0.66 (0.58, 0.74)	*	0.41 (0.37, 0.44)	0.51 (0.47, 0.54)	**
	≥ 25	0.54 (0.48, 0.60)	0.65 (0.56, 0.74)	*	0.48 (0.46, 0.50)	0.60 (0.57, 0.62)	**
Cigarettes per Day	> 25	0.54 (0.47, 0.61)	0.74 (0.65, 0.82)	**	0.45 (0.43, 0.48)	0.57 (0.53, 0.60)	**
	≤ 25	0.51 (0.43, 0.60)	0.59 (0.51, 0.67)		0.48 (0.45, 0.50)	0.56 (0.53, 0.58)	**
Lived w/ Smoker	False	0.51 (0.35, 0.67)	0.57 (0.35, 0.79)		0.46 (0.42, 0.50)	0.53 (0.44, 0.63)	
	True	0.53 (0.47, 0.59)	0.67 (0.60, 0.73)	**	0.46 (0.44, 0.48)	0.56 (0.54, 0.58)	**
Pneumonia Diag.	False	0.56 (0.50, 0.61)	0.68 (0.61, 0.75)	*	0.49 (0.47, 0.51)	0.58 (0.56, 0.61)	**
	True	0.40 (0.28, 0.53)	0.64 (0.54, 0.75)	**	0.35 (0.31, 0.39)	0.51 (0.47, 0.55)	**

Table 11: The top 10 characteristics with the largest prevalence difference between White and Black participants, and the AUROC scores of the Venkadesh21 model between these racial groups isolating for them.

Confounder	Subset	White			AUROC	Mal	Ben	Black			AUROC	p
		Mal	Ben	Total %				Total %	Black			
Cigarettes per Day	≤ 25	246	2610	51.7	0.88 (0.86, 0.90)	20	127	78.2	0.77 (0.67, 0.87)	.08		
	> 25	284	2383	48.3	0.90 (0.89, 0.92)	8	33	21.8	0.94 (0.85, 1.00)	.50		
Pack-Years	≤ 55	249	2877	56.6	0.88 (0.86, 0.90)	23	125	78.7	0.79 (0.69, 0.88)	.10		
	> 55	281	2116	43.4	0.90 (0.88, 0.91)	5	35	21.3	0.93 (0.83, 1.00)	.63		
Hypertension Diag.	True	196	1617	32.8	0.87 (0.84, 0.90)	16	86	54.3	0.73 (0.61, 0.85)	.04		
	False	329	3373	67.0	0.90 (0.89, 0.92)	12	74	45.7	0.93 (0.87, 0.98)	.60		
Current Smoker	False	247	2542	50.5	0.89 (0.87, 0.91)	11	48	31.4	0.88 (0.77, 0.96)	.80		
	True	283	2451	49.5	0.89 (0.87, 0.91)	17	112	68.6	0.76 (0.62, 0.88)	.05		
Smoked Pipe	True	132	1127	22.8	0.90 (0.87, 0.92)	5	12	9.0	0.93 (0.77, 1.00)	.75		
	False	397	3837	76.7	0.89 (0.87, 0.91)	23	145	89.4	0.80 (0.70, 0.89)	.11		
Sex	Female	218	2084	41.7	0.89 (0.87, 0.91)	15	88	54.8	0.84 (0.75, 0.92)	.40		
	Male	312	2909	58.3	0.89 (0.87, 0.91)	13	72	45.2	0.81 (0.66, 0.93)	.24		
Diabetes Diag.	True	50	412	8.4	0.90 (0.86, 0.94)	4	31	18.6	0.67 (0.32, 1.00)	.11		
	False	480	4578	91.6	0.89 (0.88, 0.90)	24	129	81.4	0.83 (0.74, 0.91)	.26		
Height	> 68	248	2389	47.7	0.89 (0.87, 0.91)	11	60	37.8	0.78 (0.61, 0.93)	.19		
	≤ 68	282	2604	52.3	0.89 (0.87, 0.91)	17	100	62.2	0.84 (0.76, 0.92)	.36		
Work - Farming	False	485	4358	87.7	0.89 (0.88, 0.91)	26	156	96.8	0.81 (0.71, 0.88)	.09		
	True	45	635	12.3	0.90 (0.85, 0.94)	2	4	3.2	0.99 (1.00, 1.00)	.05		
Age at Smoking Onset	≤ 16	320	2735	55.3	0.89 (0.87, 0.91)	10	79	47.3	0.88 (0.80, 0.95)	.90		
	> 16	210	2258	44.7	0.90 (0.87, 0.92)	18	81	52.7	0.78 (0.66, 0.89)	.07		

Table 12: Sensitivity and Specificity at specific thresholds (with 95% confidence intervals) for the Venkadesh21 model between between White and Black participants, isolating for the top 10 characteristics with the largest prevalence difference between racial groups. Single asterisk (*) = metric of one subgroup is outside the CI of the other. Double asterisks (**) = CIs do not intersect.

Confounder	Subset	Sensitivity (90% Overall Specificity)			Specificity (90% Overall Sensitivity)		
		White	Black	CI	White	Black	CI
Cigarettes per Day	> 25	0.72 (0.66, 0.77)	0.75 (0.40, 1.00)	0.66 (0.64, 0.68)	0.70 (0.53, 0.85)		
	≤ 25	0.65 (0.60, 0.71)	0.25 (0.07, 0.44)	** 0.66 (0.64, 0.68)	0.74 (0.67, 0.81)	*	
Pack-Years	> 55	0.71 (0.65, 0.76)	0.60 (0.00, 1.00)	0.65 (0.63, 0.67)	0.71 (0.54, 0.85)		
	≤ 55	0.67 (0.61, 0.73)	0.35 (0.16, 0.55)	** 0.67 (0.65, 0.69)	0.74 (0.66, 0.82)		
Hypertension Diag.	False	0.71 (0.66, 0.76)	0.67 (0.36, 0.92)	0.67 (0.65, 0.69)	0.72 (0.61, 0.82)		
	True	0.65 (0.58, 0.72)	0.19 (0.00, 0.40)	** 0.64 (0.62, 0.66)	0.74 (0.65, 0.84)	*	
Current Smoker	False	0.67 (0.60, 0.72)	0.36 (0.10, 0.67)	*	0.67 (0.65, 0.68)	0.77 (0.65, 0.89)	
	True	0.71 (0.65, 0.76)	0.41 (0.17, 0.67)	*	0.65 (0.63, 0.67)	0.71 (0.63, 0.80)	
Smoked Pipe	False	0.70 (0.65, 0.74)	0.43 (0.23, 0.65)	** 0.66 (0.65, 0.68)	0.71 (0.64, 0.78)		
	True	0.65 (0.57, 0.72)	0.20 (0.00, 0.67)	0.65 (0.63, 0.68)	0.92 (0.73, 1.00)	**	
Sex	Female	0.72 (0.66, 0.78)	0.40 (0.17, 0.67)	*	0.68 (0.66, 0.70)	0.73 (0.63, 0.82)	
	Male	0.66 (0.61, 0.71)	0.38 (0.12, 0.67)	0.65 (0.63, 0.66)	0.74 (0.64, 0.84)		
Diabetes Diag.	False	0.69 (0.64, 0.73)	0.38 (0.18, 0.57)	** 0.66 (0.65, 0.67)	0.73 (0.65, 0.80)		
	True	0.72 (0.59, 0.84)	0.50 (0.00, 1.00)	0.66 (0.61, 0.70)	0.74 (0.58, 0.88)		
Height	> 68	0.66 (0.60, 0.72)	0.36 (0.10, 0.70)	0.64 (0.62, 0.66)	0.77 (0.65, 0.86)	*	
	≤ 68	0.71 (0.66, 0.76)	0.41 (0.17, 0.67)	*	0.68 (0.66, 0.70)	0.71 (0.62, 0.79)	
Work - Farming	False	0.69 (0.64, 0.73)	0.38 (0.19, 0.57)	** 0.66 (0.65, 0.68)	0.72 (0.65, 0.78)		
	True	0.71 (0.56, 0.84)	0.50 (0.00, 1.00)	0.64 (0.61, 0.68)	1.00 (1.00, 1.00)	**	
Age at Smoking Onset	> 16	0.73 (0.67, 0.79)	0.39 (0.17, 0.63)	** 0.67 (0.65, 0.69)	0.75 (0.66, 0.84)		
	≤ 16	0.66 (0.61, 0.72)	0.40 (0.12, 0.71)	0.65 (0.64, 0.67)	0.71 (0.61, 0.81)		

Table 13: The top 10 characteristics with the largest prevalence difference between high and low BMI participants, and the AUROC scores of the Sybil (Year 1) model between BMI groups isolating for them.

Confounder	Subset	< 25			AUROC	Mal	Ben	Total %	≥ 25			AUROC	p
		Mal	Ben	Total %					Mal	Ben	Total %		
Weight	> 180	10	90	5.3	0.93 (0.83, 0.99)	237	2479	67.7	0.84 (0.81, 0.87)	11.9	.12		
	≤ 180	199	1600	94.7	0.81 (0.78, 0.84)	135	1161	32.3	0.89 (0.86, 0.92)	32.1	.002		
Current Smoker	False	74	642	37.7	0.82 (0.76, 0.87)	193	2021	55.2	0.85 (0.82, 0.88)	55.2	.30		
	True	135	1048	62.3	0.81 (0.77, 0.86)	179	1619	44.8	0.86 (0.84, 0.89)	44.8	.07		
Sex	Female	117	879	52.4	0.85 (0.81, 0.89)	127	1347	36.7	0.90 (0.87, 0.93)	36.7	.11		
	Male	92	811	47.6	0.76 (0.70, 0.82)	245	2293	63.3	0.83 (0.80, 0.86)	63.3	.03		
Emphysema in Scan	True	103	789	47.0	0.78 (0.73, 0.83)	161	1103	31.5	0.81 (0.77, 0.85)	31.5	.44		
	False	106	901	53.0	0.84 (0.79, 0.89)	211	2537	68.5	0.88 (0.86, 0.91)	68.5	.10		
Hypertension Diag.	True	62	397	24.2	0.80 (0.73, 0.86)	161	1373	38.2	0.82 (0.79, 0.85)	38.2	.55		
	False	143	1292	75.6	0.82 (0.78, 0.85)	209	2265	61.7	0.88 (0.85, 0.90)	61.7	.02		
Height	> 68	71	680	39.5	0.77 (0.70, 0.83)	196	1820	50.2	0.82 (0.78, 0.85)	50.2	.19		
	≤ 68	138	1010	60.5	0.84 (0.81, 0.88)	176	1820	49.8	0.89 (0.87, 0.92)	49.8	.04		
Total Years of Smoking	> 40	142	983	59.2	0.79 (0.75, 0.84)	248	1782	50.6	0.86 (0.84, 0.88)	50.6	.009		
	≤ 40	67	707	40.8	0.85 (0.80, 0.90)	124	1858	49.4	0.84 (0.80, 0.88)	49.4	.69		
Smoked Pipe	False	174	1403	83.0	0.83 (0.80, 0.87)	262	2736	74.7	0.86 (0.84, 0.89)	74.7	.15		
	True	34	280	16.5	0.74 (0.63, 0.84)	109	878	24.6	0.83 (0.79, 0.87)	24.6	.09		
Diabetes Diag.	True	6	62	3.6	0.99 (1.00, 1.00)	51	426	11.9	0.82 (0.75, 0.88)	11.9	< .001		
	False	202	1625	96.2	0.81 (0.77, 0.84)	321	3214	88.1	0.86 (0.84, 0.88)	88.1	.01		
Smoked Cigars	False	181	1446	85.7	0.83 (0.80, 0.87)	289	2822	77.5	0.86 (0.83, 0.89)	77.5	.23		
	True	27	238	14.0	0.70 (0.59, 0.81)	82	801	22.0	0.83 (0.79, 0.88)	22.0	.02		

Table 14: Sensitivity and Specificity at specific thresholds (with 95% confidence intervals) for the Sybil (Year 1) model between high and low BMI participants, isolating for the top 10 characteristics with the largest prevalence difference between subgroups. Single asterisk (*) = metric of one subgroup is outside the CI of the other. Double asterisks (**) = CIs do not intersect.

Confounder	Subset	Sensitivity (90% Overall Specificity)			Specificity (90% Overall Sensitivity)		
		≥ 25	< 25	CI	≥ 25	< 25	CI
Weight	> 180	0.56 (0.50, 0.62)	0.80 (0.50, 1.00)	0.51 (0.49, 0.53)	0.54 (0.44, 0.64)		
	≤ 180	0.61 (0.52, 0.69)	0.58 (0.51, 0.64)	0.55 (0.52, 0.58)	0.45 (0.43, 0.48)	**	
Current Smoker	False	0.57 (0.50, 0.64)	0.57 (0.45, 0.69)	0.52 (0.50, 0.55)	0.50 (0.46, 0.54)		
	True	0.59 (0.52, 0.66)	0.60 (0.52, 0.68)	0.53 (0.50, 0.55)	0.43 (0.40, 0.46)	**	
Sex	Female	0.65 (0.57, 0.74)	0.66 (0.57, 0.75)	0.60 (0.57, 0.62)	0.51 (0.47, 0.54)	**	
	Male	0.54 (0.48, 0.60)	0.50 (0.40, 0.61)	0.48 (0.46, 0.50)	0.41 (0.37, 0.44)	**	
Emphysema in Scan	False	0.60 (0.54, 0.66)	0.60 (0.50, 0.70)	0.56 (0.54, 0.58)	0.51 (0.48, 0.55)	*	
	True	0.55 (0.47, 0.63)	0.57 (0.48, 0.67)	0.44 (0.42, 0.47)	0.40 (0.36, 0.43)	*	
Hypertension Diag.	False	0.63 (0.57, 0.70)	0.56 (0.49, 0.64)	0.55 (0.53, 0.57)	0.46 (0.43, 0.49)	**	
	True	0.51 (0.43, 0.58)	0.65 (0.53, 0.77)	*	0.48 (0.46, 0.51)	0.46 (0.41, 0.51)	
Height	> 68	0.54 (0.46, 0.61)	0.49 (0.38, 0.61)	0.48 (0.45, 0.50)	0.39 (0.35, 0.43)	**	
	≤ 68	0.62 (0.55, 0.70)	0.64 (0.55, 0.72)	0.57 (0.55, 0.59)	0.50 (0.48, 0.54)	**	
Total Years of Smoking	> 40	0.59 (0.53, 0.65)	0.59 (0.52, 0.67)	0.49 (0.46, 0.51)	0.42 (0.39, 0.45)	**	
	≤ 40	0.56 (0.47, 0.64)	0.58 (0.47, 0.70)	0.56 (0.54, 0.58)	0.51 (0.48, 0.55)	*	
Smoked Pipe	False	0.60 (0.54, 0.67)	0.61 (0.55, 0.69)	0.54 (0.52, 0.56)	0.47 (0.44, 0.49)	**	
	True	0.51 (0.42, 0.61)	0.47 (0.30, 0.65)	0.49 (0.45, 0.52)	0.42 (0.36, 0.47)	*	
Diabetes Diag.	False	0.57 (0.52, 0.63)	0.58 (0.51, 0.65)	0.53 (0.51, 0.54)	0.46 (0.43, 0.48)	**	
	True	0.61 (0.47, 0.72)	1.00 (1.00, 1.00)	**	0.52 (0.48, 0.57)	0.55 (0.42, 0.68)	
Smoked Cigars	False	0.60 (0.54, 0.66)	0.62 (0.55, 0.68)	0.53 (0.51, 0.55)	0.46 (0.44, 0.49)	**	
	True	0.50 (0.39, 0.60)	0.41 (0.22, 0.60)	0.51 (0.48, 0.55)	0.42 (0.36, 0.48)	*	

Table 15: The top 10 characteristics with the largest prevalence difference between high and low BMI participants, and the AUROC scores of the PanCan2b model between BMI groups isolating for them.

Confounder	Subset	< 25			AUROC	Mal	Ben	Total %	≥ 25			AUROC	p
		Mal	Ben	Total %					Mal	Ben	Total %		
Weight	> 180	10	90	5.3	0.85 (0.68, 0.99)	237	2479	67.7	0.80 (0.77, 0.83)	46	.46	< .001	
	≤ 180	199	1600	94.7	0.73 (0.69, 0.76)	135	1161	32.3	0.82 (0.79, 0.85)	46	.46		
Current Smoker	False	74	642	37.7	0.76 (0.70, 0.82)	193	2021	55.2	0.80 (0.77, 0.83)	24	.24	.002	
	True	135	1048	62.3	0.72 (0.67, 0.77)	179	1619	44.8	0.81 (0.78, 0.84)	24	.24		
Sex	Female	117	879	52.4	0.74 (0.69, 0.79)	127	1347	36.7	0.81 (0.78, 0.85)	46	.02	.01	
	Male	92	811	47.6	0.73 (0.67, 0.78)	245	2293	63.3	0.81 (0.79, 0.84)	46	.01		
Emphysema in Scan	True	103	789	47.0	0.68 (0.62, 0.73)	161	1103	31.5	0.80 (0.76, 0.83)	24	< .001	.02	
	False	106	901	53.0	0.78 (0.74, 0.83)	211	2537	68.5	0.81 (0.78, 0.83)	24	.43		
Hypertension Diag.	True	62	397	24.2	0.70 (0.63, 0.77)	161	1373	38.2	0.78 (0.74, 0.82)	24	.05	.005	
	False	143	1292	75.6	0.74 (0.70, 0.78)	209	2265	61.7	0.82 (0.80, 0.85)	24	.005		
Height	> 68	71	680	39.5	0.70 (0.64, 0.77)	196	1820	50.2	0.81 (0.78, 0.84)	24	.004	.05	
	≤ 68	138	1010	60.5	0.75 (0.71, 0.79)	176	1820	49.8	0.81 (0.78, 0.84)	24	.05		
Total Years of Smoking	> 40	142	983	59.2	0.69 (0.64, 0.74)	248	1782	50.6	0.79 (0.76, 0.82)	24	< .001	.56	
	≤ 40	67	707	40.8	0.80 (0.74, 0.86)	124	1858	49.4	0.82 (0.79, 0.85)	24	.56		
Smoked Pipe	False	174	1403	83.0	0.73 (0.69, 0.77)	262	2736	74.7	0.81 (0.79, 0.84)	24	.002	.16	
	True	34	280	16.5	0.72 (0.63, 0.81)	109	878	24.6	0.80 (0.76, 0.84)	24	.16		
Diabetes Diag.	True	6	62	3.6	0.96 (0.91, 1.00)	51	426	11.9	0.85 (0.80, 0.90)	24	.06	.001	
	False	202	1625	96.2	0.72 (0.69, 0.76)	321	3214	88.1	0.80 (0.78, 0.83)	24	.001		
Smoked Cigars	False	181	1446	85.7	0.74 (0.70, 0.78)	289	2822	77.5	0.80 (0.78, 0.83)	24	.01	.008	
	True	27	238	14.0	0.66 (0.55, 0.77)	82	801	22.0	0.83 (0.79, 0.87)	24	.008		

Table 16: The top 10 characteristics with the largest prevalence difference between have graduated high school or higher and those who have not, and the AUROC scores of the PanCan2b model between these subgroups isolating for them.

Confounder	Subset	< HS			≥ HS			p		
		Mal	Ben	Total %	AUROC	Mal	Ben	Total %		
Age at Smoking Onset	≤ 16	30	291	80.0	0.78 (0.69, 0.86)	309	2580	53.5	0.77 (0.74, 0.79)	.91
	> 16	11	69	20.0	0.78 (0.62, 0.92)	217	2293	46.5	0.81 (0.78, 0.83)	.72
Total Years of Smoking	≤ 40	10	87	24.2	0.70 (0.49, 0.88)	173	2435	48.3	0.83 (0.80, 0.85)	.15
	> 40	31	273	75.8	0.81 (0.73, 0.87)	353	2438	51.7	0.75 (0.73, 0.78)	.24
Work w/o Mask	True	14	158	42.9	0.70 (0.55, 0.85)	123	1189	24.3	0.77 (0.73, 0.82)	.38
	False	27	202	57.1	0.83 (0.75, 0.91)	403	3684	75.7	0.79 (0.77, 0.81)	.35
Age	> 61	26	257	70.6	0.81 (0.71, 0.88)	326	2646	55.0	0.76 (0.73, 0.78)	.36
	≤ 61	15	103	29.4	0.77 (0.63, 0.88)	200	2227	45.0	0.81 (0.78, 0.84)	.51
Pack-Years	≤ 55	24	167	47.6	0.75 (0.65, 0.84)	254	2866	57.8	0.81 (0.78, 0.83)	.32
	> 55	17	193	52.4	0.83 (0.70, 0.92)	272	2007	42.2	0.76 (0.73, 0.79)	.30
Worked w/ Smoker	True	34	283	79.1	0.76 (0.67, 0.83)	467	4272	87.8	0.79 (0.77, 0.81)	.52
	False	6	73	19.7	0.92 (0.85, 0.97)	57	561	11.4	0.76 (0.70, 0.82)	.07
Sex	Female	14	121	33.7	0.81 (0.68, 0.92)	227	2059	42.3	0.78 (0.75, 0.81)	.70
	Male	27	239	66.3	0.78 (0.69, 0.86)	299	2814	57.7	0.79 (0.77, 0.82)	.79
Work - Welding	False	36	308	85.8	0.79 (0.71, 0.86)	491	4608	94.4	0.78 (0.76, 0.80)	.91
	True	5	52	14.2	0.76 (0.48, 1.00)	35	265	5.6	0.83 (0.75, 0.89)	.59
Diameter (mm)	> 6	39	247	71.3	0.74 (0.66, 0.81)	473	2917	62.8	0.73 (0.71, 0.75)	.90
	≤ 6	2	113	28.7	0.54 (0.15, 0.91)	53	1956	37.2	0.66 (0.59, 0.73)	.56
Current Smoker	False	21	146	41.6	0.72 (0.58, 0.83)	238	2469	50.1	0.80 (0.77, 0.83)	.18
	True	20	214	58.4	0.84 (0.76, 0.91)	288	2404	49.9	0.77 (0.74, 0.80)	.19

Table 17: Sensitivity and Specificity at specific thresholds (with 95% confidence intervals) for the Venkadesh21 model between participants who have graduated high school or higher and those who have not, isolating for the top 10 characteristics with the largest prevalence difference between subgroups. Single asterisk (*) = metric of one subgroup is outside the CI of the other. Double asterisks (**) = CIs do not intersect.

Confounder	Subset	Sensitivity (90% Overall Specificity)			Specificity (90% Overall Sensitivity)		
		> HS	≥ HS	< HS	CI	≥ HS	< HS
Age at Smoking Onset	> 16	0.71 (0.65, 0.77)	0.73 (0.44, 1.00)		0.67 (0.65, 0.69)	0.55 (0.43, 0.66)	*
	≤ 16	0.67 (0.61, 0.72)	0.67 (0.50, 0.84)		0.67 (0.65, 0.69)	0.55 (0.49, 0.61)	**
Total Years of Smoking	> 40	0.70 (0.65, 0.75)	0.71 (0.56, 0.86)		0.65 (0.63, 0.67)	0.57 (0.51, 0.63)	**
	≤ 40	0.65 (0.57, 0.72)	0.60 (0.25, 0.90)		0.69 (0.67, 0.71)	0.48 (0.38, 0.58)	**
Work w/o Mask	False	0.70 (0.65, 0.74)	0.70 (0.51, 0.87)		0.67 (0.66, 0.69)	0.56 (0.50, 0.63)	**
	True	0.64 (0.56, 0.72)	0.64 (0.38, 0.90)		0.68 (0.65, 0.70)	0.53 (0.45, 0.61)	**
Age	> 61	0.71 (0.66, 0.75)	0.69 (0.50, 0.87)		0.65 (0.63, 0.66)	0.56 (0.50, 0.62)	**
	≤ 61	0.65 (0.58, 0.72)	0.67 (0.42, 0.90)		0.70 (0.68, 0.72)	0.53 (0.44, 0.63)	**
Pack-Years	> 55	0.71 (0.66, 0.76)	0.71 (0.44, 0.91)		0.65 (0.63, 0.68)	0.59 (0.52, 0.66)	
	≤ 55	0.65 (0.59, 0.71)	0.67 (0.48, 0.85)		0.69 (0.67, 0.70)	0.50 (0.43, 0.58)	**
Worked w/ Smoker	False	0.61 (0.49, 0.74)	0.50 (0.00, 1.00)		0.66 (0.62, 0.70)	0.55 (0.44, 0.67)	
	True	0.69 (0.65, 0.73)	0.74 (0.58, 0.88)		0.67 (0.66, 0.69)	0.55 (0.49, 0.61)	**
Sex	Female	0.70 (0.64, 0.76)	0.93 (0.78, 1.00)	**	0.69 (0.67, 0.71)	0.59 (0.50, 0.67)	**
	Male	0.68 (0.62, 0.72)	0.56 (0.38, 0.73)		0.66 (0.64, 0.68)	0.53 (0.47, 0.59)	**
Work - Welding	False	0.68 (0.64, 0.73)	0.67 (0.49, 0.81)		0.67 (0.66, 0.69)	0.56 (0.51, 0.62)	**
	True	0.69 (0.54, 0.84)	0.80 (0.33, 1.00)		0.68 (0.62, 0.73)	0.46 (0.32, 0.60)	**
Diameter (mm)	> 6	0.74 (0.70, 0.78)	0.69 (0.53, 0.83)		0.51 (0.50, 0.53)	0.44 (0.38, 0.51)	*
	≤ 6	0.23 (0.12, 0.35)	0.50 (0.00, 1.00)		0.91 (0.89, 0.92)	0.79 (0.71, 0.86)	**
Current Smoker	False	0.69 (0.63, 0.75)	0.52 (0.31, 0.74)		0.68 (0.66, 0.70)	0.52 (0.44, 0.60)	**
	True	0.68 (0.62, 0.74)	0.85 (0.68, 1.00)		0.66 (0.65, 0.68)	0.57 (0.50, 0.64)	**

Table 18: Sensitivity and Specificity at specific thresholds (with 95% confidence intervals) for the Sybil Year 1 model between participants who have graduated high school or higher and those who have not, isolating for the top 10 characteristics with the largest prevalence difference between subgroups. Single asterisk (*) = metric of one subgroup is outside the CI of the other. Double asterisks (**) = CIs do not intersect.

Confounder	Subset	Sensitivity (90% Overall Specificity)			Specificity (90% Overall Sensitivity)		
		\geq HS	< HS	CI	\geq HS	< HS	CI
Age at Smoking Onset	> 16	0.62 (0.56, 0.68)	0.55 (0.22, 0.83)	0.52 (0.50, 0.54)	0.39 (0.28, 0.51)	*	
	\leq 16	0.56 (0.51, 0.62)	0.57 (0.38, 0.74)	0.51 (0.49, 0.53)	0.36 (0.30, 0.41)	**	
Total Years of Smoking	> 40	0.59 (0.53, 0.64)	0.68 (0.52, 0.84)	0.47 (0.45, 0.49)	0.35 (0.29, 0.40)	**	
	\leq 40	0.59 (0.51, 0.66)	0.20 (0.00, 0.50)	**	0.55 (0.54, 0.57)	0.41 (0.31, 0.51)	**
Work w/o Mask	False	0.61 (0.56, 0.66)	0.56 (0.38, 0.75)	0.53 (0.51, 0.55)	0.39 (0.32, 0.45)	**	
	True	0.51 (0.42, 0.60)	0.57 (0.33, 0.83)	0.46 (0.43, 0.49)	0.34 (0.26, 0.41)	**	
Age	> 61	0.61 (0.55, 0.66)	0.65 (0.45, 0.83)	0.46 (0.44, 0.48)	0.35 (0.28, 0.41)	**	
	\leq 61	0.55 (0.48, 0.62)	0.40 (0.17, 0.64)	0.58 (0.55, 0.60)	0.41 (0.32, 0.50)	**	
Pack-Years	> 55	0.61 (0.55, 0.66)	0.65 (0.38, 0.87)	0.48 (0.46, 0.50)	0.33 (0.26, 0.39)	**	
	\leq 55	0.57 (0.51, 0.63)	0.50 (0.31, 0.70)	0.54 (0.52, 0.55)	0.41 (0.33, 0.48)	**	
Worked w/ Smoker	False	0.49 (0.37, 0.61)	0.50 (0.00, 1.00)	0.55 (0.51, 0.59)	0.42 (0.31, 0.54)	*	
	True	0.60 (0.56, 0.64)	0.59 (0.42, 0.74)	0.51 (0.49, 0.52)	0.35 (0.30, 0.41)	**	
Sex	Female	0.64 (0.58, 0.71)	0.79 (0.55, 1.00)	0.57 (0.54, 0.59)	0.42 (0.33, 0.50)	**	
	Male	0.55 (0.49, 0.60)	0.44 (0.26, 0.63)	0.47 (0.46, 0.49)	0.33 (0.28, 0.40)	**	
Work - Welding	False	0.59 (0.54, 0.63)	0.56 (0.38, 0.73)	0.52 (0.51, 0.53)	0.39 (0.33, 0.44)	**	
	True	0.54 (0.38, 0.71)	0.60 (0.00, 1.00)	0.38 (0.33, 0.44)	0.23 (0.12, 0.35)	*	
Diameter (mm)	> 6	0.64 (0.60, 0.68)	0.59 (0.44, 0.74)	0.38 (0.36, 0.39)	0.26 (0.20, 0.32)	**	
	\leq 6	0.11 (0.03, 0.20)	0.00 (0.00, 0.00)	**	0.72 (0.70, 0.74)	0.59 (0.50, 0.68)	**
Current Smoker	False	0.59 (0.53, 0.65)	0.43 (0.21, 0.64)	0.53 (0.51, 0.55)	0.35 (0.27, 0.43)	**	
	True	0.59 (0.53, 0.64)	0.70 (0.48, 0.88)	0.50 (0.48, 0.52)	0.37 (0.31, 0.44)	**	

Table 19: Sensitivity and Specificity at specific thresholds (with 95% confidence intervals) for the PanCan2b model between participants who have graduated high school or higher and those who have not, isolating for the top 10 characteristics with the largest prevalence difference between subgroups. Single asterisk (*) = metric of one subgroup is outside the CI of the other. Double asterisks (**) = CIs do not intersect.

Confounder	Subset	Sensitivity (90% Overall Specificity)			Specificity (90% Overall Sensitivity)		
		> HS	≥ HS	< HS	≥ HS	< HS	CI
Age at Smoking Onset	> 16	0.40 (0.34, 0.47)	0.45 (0.17, 0.75)		0.44 (0.42, 0.46)	0.26 (0.16, 0.36)	**
	≤ 16	0.38 (0.32, 0.43)	0.40 (0.23, 0.59)		0.46 (0.44, 0.48)	0.38 (0.32, 0.43)	**
Total Years of Smoking	> 40	0.37 (0.32, 0.42)	0.45 (0.28, 0.64)		0.41 (0.39, 0.43)	0.36 (0.31, 0.42)	
	≤ 40	0.42 (0.35, 0.49)	0.30 (0.00, 0.62)		0.49 (0.47, 0.51)	0.33 (0.24, 0.43)	**
Work w/o Mask	False	0.39 (0.34, 0.44)	0.48 (0.30, 0.68)		0.44 (0.43, 0.46)	0.40 (0.34, 0.47)	
	True	0.36 (0.28, 0.44)	0.29 (0.08, 0.56)		0.48 (0.46, 0.51)	0.30 (0.23, 0.37)	**
Age	> 61	0.39 (0.34, 0.44)	0.42 (0.22, 0.63)		0.40 (0.38, 0.42)	0.33 (0.27, 0.39)	*
	≤ 61	0.38 (0.31, 0.45)	0.40 (0.15, 0.67)		0.52 (0.50, 0.54)	0.42 (0.33, 0.50)	*
Pack-Years	> 55	0.37 (0.31, 0.43)	0.35 (0.14, 0.60)		0.45 (0.43, 0.47)	0.38 (0.31, 0.45)	*
	≤ 55	0.41 (0.34, 0.47)	0.46 (0.28, 0.67)		0.46 (0.44, 0.47)	0.33 (0.26, 0.41)	**
Worked w/ Smoker	False	0.40 (0.27, 0.54)	0.50 (0.00, 1.00)		0.43 (0.39, 0.47)	0.45 (0.33, 0.56)	
	True	0.39 (0.34, 0.43)	0.41 (0.24, 0.58)		0.45 (0.44, 0.47)	0.33 (0.28, 0.39)	**
Sex	Female	0.46 (0.39, 0.52)	0.64 (0.36, 0.88)		0.37 (0.35, 0.40)	0.26 (0.18, 0.34)	**
	Male	0.33 (0.28, 0.39)	0.30 (0.14, 0.47)		0.51 (0.49, 0.53)	0.41 (0.35, 0.47)	**
Work - Welding	False	0.38 (0.33, 0.42)	0.42 (0.25, 0.57)		0.45 (0.44, 0.46)	0.36 (0.31, 0.41)	**
	True	0.49 (0.31, 0.65)	0.40 (0.00, 1.00)		0.49 (0.43, 0.55)	0.33 (0.20, 0.46)	*
Diameter (mm)	> 6	0.43 (0.38, 0.47)	0.44 (0.28, 0.60)		0.15 (0.14, 0.16)	0.11 (0.08, 0.15)	
	≤ 6	0.00 (0.00, 0.00)	0.00 (0.00, 0.00)		0.90 (0.89, 0.92)	0.88 (0.83, 0.94)	
Current Smoker	False	0.39 (0.33, 0.45)	0.38 (0.19, 0.59)		0.45 (0.43, 0.47)	0.33 (0.26, 0.41)	**
	True	0.39 (0.33, 0.44)	0.45 (0.24, 0.68)		0.45 (0.44, 0.47)	0.37 (0.31, 0.44)	*